T.R.
ERCIYES UNIVERSITY
GRADUATE SCHOOL OF NATURAL AND APPLIED SCIENCES
DIVISION OF MECHANICAL ENGINEERING

DELAMINATION ANALYSIS OF FUNCTIONALLY GRADED MATERIALS USİNG CARRERA UNIFIED FORMULATION AND COHESIVE ZONE MODEL

Written by:
Mohammed Nasseer Abdulrahman MOHAMMED

Supervisors
Assoc. Prof. Munise Didem DEMIRBAS
Prof. Erasmo CARRERA

Master's Degree Thesis

July 2023
KAYSERI

T.R.
ERCIYES UNIVERSITY
GRADUATE SCHOOL OF NATURAL AND APPLIED SCIENCES
DIVISION OF MECHANICAL ENGINEERING

DELAMINATION ANALYSIS OF FUNCTIONALLY GRADED MATERIALS USING CARRERA UNIFIED FORMULATION AND COHESIVE ZONE MODEL

(Master's Degree Thesis)

Written by:
Mohammed Nasseer Abdulrahman MOHAMMED

Supervisors
Assoc. Prof. Munise Didem DEMIRBAS
Prof. Erasmo CARRERA

July 2023
KAYSERI

COMPLIANCE WITH SCIENTIFIC ETHICS

I declare that all information in this study has been obtained in accordance with academic and ethical rules. At the same time, as required by these rules and conduct, I declare that I have fully cited and referenced all material and results that are not at the core of this work.

Mohammed Nasseer Abdulrahman MOHAMMED

İmza

The Master Thesis named **"Delamination Analysis of Functionally Graded Materials using Carrera Unified Formulation and Cohesive Zone Model"** has been prepared in accordance with the Erciyes University Graduate Thesis Proposal and Thesis Writing Directive.

Prepared	**Supervisor**
Mohammed Nasseer Abdulrahman MOHAMMED	Assoc. Prof. Munise Didem DEMIRBAS
signature	signature

Head of Mechanic Division

Prof. S. Orhan Akansu İmza

APPRECIATION

I would like to express my heartfelt gratitude to my 1st supervisor, Assoc. Prof. Munise Didem DEMIRBAS, my 2nd supervisor, Prof. Erasmo Carrera, and Dr. Riccardo Augello for their invaluable guidance, unwavering support, and dedication throughout my thesis working time. Their expertise and constructive feedback played a pivotal role in shaping the direction and success of my research. I am privileged to have had the opportunity to work under their supervision. Thank you for your unwavering support and encouragement.

Mohammed Nasseer Abdulrahman MOHAMMED

July 2023, KAYSERİ

DELAMINATION ANALYSIS OF FUNCTIONALLY GRADED MATERIALS USING CARRERA UNIFIED FORMULATION AND COHESIVE ZONE MODEL

Mohammed Nasseer Abdulrahman MOHAMMED

Erciyes University, Graduate School of Natural and Applied Sciences
Master Thesis, July 2023
Supervisor: Assoc. Prof. Munise Didem DEMIRBAS and Prof. Erasmo CARRERA

ABSTRACT

This thesis presents a comprehensive investigation into the delamination behavior of Functionally Graded Materials (FGMs), incorporating Carrera Unified Formulation (CUF) and Cohesive Zone Model (CZM). FGMs, with their unique spatially varying material properties, have emerged as promising candidates for advanced engineering applications However, there are some critical concerns in these structures, such as delamination. Therefore, it is necessary to investigate the mechanical responses and failure mechanisms in detail.

The proposed numerical solution in this thesis uses CUF's efficient hierarchical formulation and the CZM's fracture mechanics. The problem to be analyzed is a ceramics-metal FGM beam of 10 layers subjected to delamination forces. The beam has one fixed end 2 opposite forces are acting on the first and last layers at the free end causing delamination. The Lagrange expansion used for the cracked beams is facilitating accurate and detailed simulations of the delamination phenomenon in FGMs as it is suitable for modeling discontinuities. CZM is also well-suited for analyzing fracture propagation in composite materials. It offers cohesive elements that handle crack initiation, propagation, and branching according to a specified traction-separation law.

Keywords: Carrera Unified Formulation, Cohesive Zone Model, Functionally Graded Materials.

FONKSİYONEL OLARAK DERECELENDİRİLMİŞ MALZEMELERİN DELAMİNASYON ANALİZİ CARRERA BİRLEŞİK FORMÜLASYONUNUN VE BİRLEŞİK BÖLGENİN KULLANILMASI MODELİ

Muhammed Nasır Abdurrahman MOHAMMED

Erciyes Üniversitesi Fen Bilimleri Enstitüsü
Yüksek Lisans Tezi, Temmuz 2023
Danışman: Doç. Prof. Munise Didem DEMİRBAŞ ve Prof. Erasmo CARRERA

ÖZET

Bu tez, katmanlara ayrılma davranışına ilişkin kapsamlı bir araştırma sunmaktadır. Carrera Birleşik Formülasyonunu içeren Fonksiyonel Derecelendirilmiş Malzemeler (FGM'ler) (CUF) ve Yapışkan Bölge Modeli (CZM). Benzersiz mekansal değişkenlikleriyle FGM'ler malzeme özellikleri ileri mühendislik için umut verici adaylar olarak ortaya çıkmıştır.

Ancak bu yapılarda bazı kritik kaygılar vardır: delaminasyon. Bu nedenle mekanik tepkilerin araştırılması ve Arıza mekanizmaları ayrıntılı olarak. Bu tezde önerilen sayısal çözüm, CUF'nin etkin hiyerarşik yapısını kullanır. formülasyonu ve CZM'nin kırılma mekaniği. Analiz edilecek problem bir seramik metalidir. Delaminasyon kuvvetlerine maruz kalan 10 katmanlı FGM kirişi. Kirişin sabit bir tane var uç 2 zıt kuvvetler serbest uçtaki ilk ve son katmanlara etki ederek delaminasyon. Çatlak kirişler için kullanılan Lagrange genişletmesi hassas hesaplamayı kolaylaştırmaktadır. ve FGM'lerdeki delaminasyon olgusunun detaylı simülasyonları, süreksizliklerin modellenmesi. CZM ayrıca kırılma yayılımını analiz etmek için de çok uygundur. kompozit malzemeler. Çatlak başlangıcını, yayılmasını, ve belirli bir çekme-ayırma yasasına göre dallanma.

Anahtar Kelimeler: Carrera Birleşik Formülasyon, Kohezif Bölge Modeli, Fonksiyonel Derecelendirilmiş Malzemeler.

CONTENTS

DELAMINATION ANALYSIS OF FUNCTIONALLY GRADED MATERIALS USING CARRERA UNIFIED FORMULATION AND COHESIVE ZONE MODEL

ABBREVIATIONS

CUF: Carrera Unıfied Formulation

CZM: Cohesive Zone Model

FGMs: Functionally Graded Materials

CM: Composite Materials

LIST OF TABLES

LIST OF FIGURES

INTRODUCTION

FGMs have emerged as a fascinating class of advanced materials with spatially varying material properties that can be adapted to meet specific engineering requirements. The gradient in material composition throughout FGM structures gives them outstanding mechanical, thermal, and chemical properties, offering enhanced performance and versatility over conventional homogeneous materials. FGMs have been the subject of extensive research in the aerospace, automotive, biomedical, and other high-performance industries [1].

The concept of FGMs traces its roots back to the late 19th and early 20th centuries when researchers began exploring the idea of materials with continuous variations in composition and properties. However, the term "Functionally Graded Materials" was officially coined in the 1980s by Japanese researchers to describe the novel class of engineering materials they were developing [2]. In the early 1980s, Dr. Miyamoto and his team at the National Aerospace Laboratory of Japan (currently Japan Aerospace Exploration Agency, JAXA) initiated research on ceramics and metal-ceramic composites with graded compositions. Their goal was to create materials that could withstand the extreme temperatures experienced during atmospheric re-entry of spacecraft. The first FGM developed by Dr. Miyamoto's team was a thermal protection system for space shuttles, where the composition of the ceramic material varied gradually from a thermal barrier to a structural material. This design allowed for effective thermal insulation and reduced thermal stresses during re-entry, significantly improving the reliability and performance of spacecraft [3].

Following this breakthrough, FGM research expanded globally, and other researchers started exploring FGM concepts for various applications. In the early years, FGMs were primarily focused on thermal protection systems for aerospace vehicles [3]. However, as

the understanding of materials science and manufacturing techniques grew, researchers began investigating a broader range of applications, including structural components, biomedical devices, and more [4-9].

Since the 1980s, there have been numerous advancements in FGM research and development. Researchers have explored different material combinations, fabrication methods, and property gradients to tailor the FGMs for specific applications due to their special properties. For instance, they enable the creation of materials with ongoing compositional, microstructural, and physical changes. This makes it possible for scientists to develop materials that may be tailored for particular uses, like thermal protection, wear resistance, and mechanical strength. Furthermore, by lowering stress concentrations and heat gradients, these kinds of materials might improve the efficiency and dependability of engineering structures. Better resistance to fatigue and crack propagation results from this. As a result, they increase the longevity of parts and buildings. FGMs are very useful in high-temperature settings, such as nuclear reactor applications or spacecraft re-entry. In order to prevent material deterioration and failure, they can efficiently manage temperature gradients and offer thermal insulation. Structures' weight can be decreased while maintaining their mechanical strength by using FGMs. The aerospace and transportation sectors depend on this. Because reduced weight can result in better fuel economy and financial savings. FGMs are a wonderful addition to the biological Applications. The same as dental implants, they are utilized in biomedicine. Due to their capacity to imitate the mechanical and thermal characteristics of genuine tissues, they can enhance the compatibility and functionality of biomedical devices. FGMs can also act as transitional areas between different materials. This may make it unnecessary to use conventional bonding methods and reduce stress concentration on surfaces. This makes it possible to create sturdy yet lightweight structures. The change in material properties upon the cross-section decreases failure probability. That’s why they are suitable for critical components in safety systems. FGMs have also the advantage of decreasing material usage and reducing waste so they are considered eco-friendly. While combining various functions in one material, FGMs also pave the way for the creation of new smart materials with enhanced sensing, actuation, and energy storage capabilities. Today, FGMs continue to be a vibrant and active area of research, with applications spanning aerospace, energy, electronics, medicine, and many other fields. The quest for innovative

and high-performance materials remains ongoing, and FGMs are expected to play an increasingly significant role in shaping the future of engineering and technology [10-27].

FGM structures must avoid delamination. Layer separation or cracking threatens composite materials, including 3D printed FGMs structural integrity and durability. Delamination can cause early failure, reduced load capacity, and poor performance in FGM-based components and structures. Understanding delamination behavior in FGMs is important for reaching their full capabilities. This needs a detailed study of delamination mechanisms, including crack initiation, propagation, and complex loading circumstances. Experimental testing is costly and time-consuming for these phenomena. Thus, numerical simulations help efficiently study FGM structures and delamination processes.

In this thesis, CUF was used to model the delamination process as a FEM scheme. For this reason, information about CUF will be given and its literature will be reviewed. CUF is an effective computational approach to mechanics and engineering. Professor Erasmo Carrera and his team introduced it, and its many benefits were noted. One of the key advantages of CUF is its ability to efficiently handle both geometric and material nonlinear situations. This makes it suitable for the analysis of structures subjected to large deformations, nonlinear material behavior, and failure simulations. By using hierarchical, optimized one-dimensional (1D) elements, CUF can achieve high accuracy in its predictions while minimizing computational costs. CUF can also adapt to structural problems. Researchers and engineers can use CUF to easily manage beams, plates, and shells. The formulation allows users to select and combine theories and methods to analyze specific engineering problems. CUF's hierarchical optimization approach is particularly useful when dealing with complex structures. It reduces computational work and time by allowing local optimization. This is especially valuable in large-scale simulations and optimization studies. Buckling, vibration, impact, delamination, and post-buckling analysis are among the many applications of CUF [68].

Delamination in composite structures can reduce their lifespan, making their use risky. Inter-laminar delamination can develop due to external stresses during the structure's

service life. Delamination - layer separation - is a common failure mode in laminated composites. This type of failure is often caused by minor incidents like debris impact or tool drops during maintenance [28].

Different numerical models have been proposed in the literature to describe the initiation, growth and propagation of cracks in materials and structures in the case of predictable deformation [29]. This is the weak zone, which is so important for composite and FGM materials. One of the most used numerical models is the Cohesive zone model. The cohesive zone model is a computational method for simulating interfaces between materials with different properties during fracture. It divides the interface into cohesive elements. Those elements represent the bonding forces. This model is beneficial because it accurately simulates crack propagation, especially in mixed-mode conditions. It also captures how material interfaces influence overall behavior. It's aids in design, research and tracking damage evolution. However, parameter calibration is crucial for accurate representation. The concept of CZM was initially introduced in the 1960s by Dugdale [30] and Barenblatt [31]. Over the years, several versions of cohesive zone and interface element models have been developed and utilized to simulate the initiation and progression of damage in various structures. These models have been particularly valuable in simulating phenomena like debonding in composite materials [32-33], delamination events in laminated composites [34,35], and failures in the adhesive bonding [36,37]. One advantage of the cohesive zone model is the description of crack initiation, growth, and propagation in materials and structures especially when the weak region is predictable such as in multilayer structures. That is because the region between the layers are weaker and expected to have the crack propagation occurred in it. These simulations help engineers design more robust and durable composite structures. CZM is also optimum for bonded structures for the same reason of multilayer structures. Therefore, it’s widely used in fracture analyses of adhesively bonded joints. Also, CZM allows mixed-mode fracture analyses, where cracks or delamination propagate under combined mode I, II, and III loading in the three directions. Another advantage is the ability to be effectively added to Finite Element Analysis (FEA). This model is performed by reading the distance between the nodes in the cohesive zone and refreshing the relative stiffness in the global stiffness matrix (according to traction-separation law) making it a powerful tool for numerical simulations of complex engineering problems involving

crack and delamination propagation. Experimental tests relevant to CZM involve physically validating the model's predictions. Key tests include the Double Cantilever Beam (DCB) and End-Notched Flexure (ENF) tests, which assess crack propagation. Mixed-Mode Bending (MMB) and Three-Point Bending tests simulate real conditions. Peel and Single-Lap Shear tests assess adhesive joints, while Wedge Splitting tests examine mixed-mode behavior. These experiments provide data for calibrating CZM parameters and confirming its accuracy in real-world scenarios. Cohesive zone model parameters can be determined through experimental tests. This means more valuable material data for fracture and delamination analyses.

The parameters gained by experimental tests are used also when developing numerical solutions based on the CZM. In the following section, the literature will contain studies on delamination and CZM. Balzani et al. [38] introduced a cohesive region finite element for three-dimensional mixed-mode delamination in unidirectional fiber-reinforced composite laminates. They stated that there are two constitutive laws in this element one of them decays linearly after delamination starts, and the other one softens exponentially. They also noted that damaged areas irreversibly lose their firmness. They presented delamination analyzes of the exponential model with numerical examples and emphasized that it is better for convergence.

Benzeggagh et al. [39] examined the predictions of cracking and delamination at different loading modes of glass/epoxy composites and expressed the results with total critical strain energy release rate and total fracture strength. With these results, they measured the mixed-mode delamination fracture toughness of unidirectional glass/epoxy composites.

Turon et al. [40] proposed a structural law in which constitutive parameters are determined to simulate gradual delamination. They presented that this structural law takes mechanical properties into account and allows coarser meshes without losing accuracy. Thus, with this law, which allows the use of finite element meshes that are 10 times thicker, they make the analysis of large-scale progressive delamination problems computationally traceable.

Eijo et al. [41] proposed a numerical method based on the Refined Zigzag Theory to model composite layer beam delamination. They stated that with this model, they were able to capture the relative displacement between layers during delamination with one-dimensional finite elements. They modeled the mechanical properties of the layers using the continuous isotropic damage model and used the modified Newton-Raphson method to solve the nonlinear problem. They showed that the onset and progression of delamination can be predicted in a beam consisting of two layers with this beam element.

Nguyen et. al. [42] developed an automated numerical method to simulate composite structure delamination that minimizes user intervention. They used the node placement algorithm from CAD data to create two- and three-dimensional isogeometric cohesive elements along the delamination. They demonstrated the effectiveness and accuracy of the approach with two- and three-dimensional examples.

Yuan et al. [43] presented a temperature-dependent micromechanical model for carbon fiber-reinforced polymer composites. They stated that they presented a modified adhesion region model by taking into account randomly distributed fibers, temperature-dependent Young's modulus, and thermal effects at the fiber/polymer interface in the model they created. As a result, they emphasized that the interface strength especially affects the mechanical behavior, while the hardness and fracture energy have a small effect.

Huang et. al [44] investigated the performance of logarithmic, exponential, and power sticky zone models (CZM) through experiments and simulations involving low-velocity impact on composite laminates. They emphasized that in the results of this study, the logarithmic rate-dependent CZM offers the closest agreement with the experimental data in terms of dynamic mechanical response and delamination damage. They noted that the power model agreed well with the experimental results, albeit with slightly less accurate dynamic response compared to the logarithmic model. They showed with this research that the logarithmic velocity-dependent CZM is optimal for low-velocity pulse simulations, followed by the power model and the exponential model.

Marulli et al. [45] analyzed potential damage mechanisms in thin-layer flexible substrate systems and presented crack propagation, interfacial delamination, and mixed-mode

mechanisms within layers. A series of tests were performed using the phase domain (PF) approach designed for hyperelastic materials. They stated that with the PF approach, the interaction between crack propagation and delamination at the interface in a two-layer composite with material mismatch can be subtly captured.

Linke et al. [46] focused on improving the calibration of cohesive zone models for fracture simulations. They also extended calibration using universally applicable criteria. They investigated the influence of factors such as deformation, applied load and crack length, input parameters, and numerical element size on the calibration of adhesion strength. With this work, they provided insights into the role of adhesion strength as a modeling parameter and provided valuable guidance for fracture predictions in structural design.

Chiachio et al. [47] presented an energy-based technique to predict the evolution of damage to aerospace materials. They used real fatigue data from an aerospace composite material and estimated how long the components would remain functional. With this technique, they developed mathematical equations based on the behavior of the material over time, using rigorous mathematical tools to handle prediction uncertainties. They emphasized that with these estimates, they can provide important information on safety and maintenance in operational contexts.

Safri et al. [48] presented an experimental study to evaluate impact damage in glass fiber-reinforced polymer (GFRP) composite plates. They performed high-velocity and low-velocity impact tests on GFRP plates of two different compositions. They revealed damage patterns such as fiber cracking and pull-out, fiber for low-velocity impact, and matrix cracking.

Kora et al. [49] investigated the effects of interlayer tension, low thickness, axial loading, and natural frequency on interlayer separation and wear of Aluminum Matrix Metal Composites. They also aimed to solve these problems by adding different reinforcement materials with specific properties to increase the durability of composite structures. They presented various characterization techniques used to assess the severity of delamination and wear in these composites.

Huang et al. [26] introduced a new approach that combines the phase domain cohesive region model (PFCZM) with the cell-based smoothed finite element method (CSFEM) to analyze the medium-scale fracture behavior of concrete. They validated their method using four nonlinear fracture criteria and showed that this method is capable of accurately simulating medium-scale fracture processes, crack topology, and load-displacement curves. They emphasized that the CSFEM-PFCZM approach they developed exhibited improved computational efficiency compared to traditional FEM methods. They also stated that with this approach, multi-scale fracture can be determined efficiently in complex materials such as semi-brittle composites.

Ekhtiyari et al. [51] investigated the effect of local separation rate on stress distribution near the crack tip, focusing on interlayer fracture resistance at high loading rates in fiber-reinforced laminated composites. They modified the tetralinear sticky region model to account for the velocity-dependent effects in dynamic delamination under Mode I loading and built the ABAQUS finite element software using a user-defined subprogram. They validated their model with experimental results and showed that their model is capable of capturing velocity effects in dynamic delamination scenarios.

Wang et al. [52] developed a technique to determine damage parameters for a cyclic cohesive zone model using crack closure experiments. They introduced the concept of equivalent separation to account for the non-uniform damage distribution along the crack path and obtained the damage parameters by digital image correlation analysis. They also developed an adaptive loop-skipping technique based on damage rate to increase computational efficiency. They compared the model predictions with experimental data and showed that the model accurately predicted fatigue crack growth rates.

Huo et al. [53] determined the traction-separation law of a cohesive zone model through experimental measurements using the digital image correlation technique. They used a double cantilever beam sample with a ductile adhesive layer and developed a semi-empirical analytical model to relate the pull-separation law to the spherical loading response. They measured the displacement distribution of the adhesive layer and determined the initial stiffness, maximum tensile stress, and damage evolution of the

CZM. They constructed a FEM that was validated according to the experimental results and compared it with the conventional linear damage evolution FE model. They demonstrated the effectiveness of CZM in correctly extracting the traction-separation law and improved the accuracy of their adhesive bond simulations.

Lecinana et al. [54] presented an efficient technique for describing the input fatigue parameters of the fatigue cohesive zone model recently developed by Dávila. In this approach, they leveraged surrogate modeling and multi-objective optimization, using experimental data from stratification tests to identify parameters that underline the phenomenological nature of the model. They also validated the model's ability to simulate both fatigue initiation and propagation using two different monotonic coupling laws with the literature.

Xu et al. [55] aimed to increase the computational efficiency in modeling the breakage of glass under low-velocity impact in laminated windshields. They proposed an intrinsic solid-shell cohesive zone model and used solid-shell elements because of their simplicity and effectiveness in representing gradual glass fracture. Thus, they stated that the computational load related to the internal force calculation is minimized. With their proposed model, they performed bending tests and impact tests with numerical simulation and validated their approach. They also emphasized that the developed method significantly reduces computation time compared to the solid element-based intrinsic cohesive zone model.

Li et al. [56] focused on developing a friction cohesive zone model (FCZM) for modeling interfacial mechanical responses in fiber/resin composites. With this new model, they calculated the sliding friction, interface separation, and coupling effects by incorporating Coulomb's friction law into the traction-separation law. They validated the proposed FCZM by constructing a finite element model of a microdroplet and compared the simulation results with the microdroplet test data. They also investigated the effect of interface friction on the macroscopic strength and stiffness of unidirectional composites. They applied FCZM to a representative volume element and performed FE analysis to simulate the mechanical behavior of the composites. They validated their results with

experimental data and emphasized that the application of friction accelerates the opening of bonds at the interface.

Yang et al. [57] worked on the development and implementation of the interfacial cohesive zone model of the coating interlayer, taking into account the properties of adhesive materials. Rather than expressing the shear stress-shear relationship through a coefficient, they took a more accurate approach that takes into account the rheological properties of the heterogeneous interlayer adhesive material. They also performed tensile and shear tests to determine the optimum adhesive material dosage and obtained characteristic curves for normal stress-displacement and shear stress-displacement. They developed a simulation method based on the cohesive zone model to capture the shear stress-displacement behavior of interlayer adhesive materials in pavement structures by dividing the shear stress-displacement curve into different stages. The results were confirmed by comparison with the experimental results.

Fu et al. [58] focused on the effect of interlayer adhesive materials on coating performance and developed an approach with an interfacial cohesive zone model to characterize the behavior of these adhesive materials. Starting from the traditional practice of expressing shear stress-shear relationships with coefficients, they adopted a more precise method that takes into account the rheological properties of these heterogeneous materials. They performed experimental tests including tensile and shear tests to determine the optimum adhesive material dosage, and from these tests, they obtained characteristic curves for normal stress-displacement and shear stress-displacement. Using curves, they prepared a simulation method based on the cohesive zone model that captures the stress-displacement subtleties of interlayer adhesive materials in pavement structures and validated by experimental results. They applied the model to a practical scenario, demonstrating that it was compatible with real-world monitoring data.

Bhandari et al. [59] conducted an extensive literature review focusing on the dynamic fracture behavior of FGMs as a result of cracking and fatigue. They thus aimed to shed light on the crack-related challenges in FGM, a topic that has received a lot of attention in recent years. In particular, they investigated the effect of material grading on critical

aspects such as crack tip stress fields, dynamic stress intensity factors, and crack propagation behavior.

Kumar et al. [60] conducted research to increase the strength and durability of stress transfer within the joints of FGMs and bonded joints. In this study, they examined the underlying causes of both cohesive and adhesive damage of FGMs. They performed nonlinear finite element simulations using the ABAQUS framework and also identified potential loss of structural integrity in a lap shear joint with a pre-embedded crack at the adherend-adhesive interface. Through these simulations, they extensively analyzed the load transfer and damage propagation and investigated variations in parameters such as shallow angle and compositional gradient exponent. They also revealed that mode II is the dominant failure mode and that the onset of debonding from the substrate center is influenced by the compositional gradient exponent.

Pascuzzo et al. [61] developed an innovative FEM approach aimed at predicting crack propagation behaviors in FGMs. They used the Moving Mesh, the Interaction Integral method (M-integral), and the Arbitrary Lagrange-Eulerian (ALE) formulation. They performed a sensitive fracture variable assessment at the crack front, including a description of crack initiation conditions and propagation direction, stress intensity factors, and T-stress. They also enabled the subtraction of fracture variables on the deforming elements as the crack front slides during propagation. They validated the effectiveness of this approach with available experimental and numerical data in the literature and demonstrated its potential to predict crack behavior in FGMs.

Han et al. [62] developed brittle fracture simulation in asphalt mixtures by introducing a Phase Field Method (PFM) as an alternative to traditional CZM. In this method, FEM was included in the solution to solve the problem of network dependence limitations in interface damage mechanics in simulating semi-brittle fracture of asphalt mixtures at low temperatures. They conducted various tests to demonstrate the model's performance and demonstrated its accuracy. They made comparisons with CZM-based simulations, considering both numerical results and computational efficiency. They also emphasized that PFM-based simulations exhibited slightly more pronounced brittleness behavior in

asphalt mixtures compared to CZM. In particular, they noted that PFM-based cohesive fracture simulations require less computational memory and time.

Muc [63] focused on the buckling behavior of unidirectional laminates and FGM structures containing single delaminations. He conducted experiments involving separation into both closed and open layers in rectangular plates and axisymmetric shells. To account for the effect of the variable material configuration of the FGM in this work, computational models including fourth-order plate/shell relationships were developed, and defect sensitivity analysis and post-buckling nonlinear analysis were performed in the experiments. He revealed that unsymmetrical FGM configurations lead to reduced buckling loads in delaminated structures and described the effects with a simple coefficient. He observed stable and unsteady variations of the strain energy release rate depending on the nature of the delamination and provided valuable information about the buckling behavior of these composite structures.

Rahimi et al. [64] developed a new particle-based computational method to simulate the dynamic propagation of cracks in FGMs subjected to dynamic loading and significant deformations. They used a unique combination of softened particle hydrodynamics and a phase domain approach to model brittle fracture in this method. They effectively simulated material separation due to extreme deformations using a meshless discretization technique. They used a hyperbolic partial differential equation for damage development in their method, thus enabling efficient open-time integration and avoiding the complexity of solving linear systems. They applied this innovative approach to challenging impact scenarios involving rapid dynamics and significant deformations and demonstrated the ability to identify material transition profiles that affect crack propagation for FGMs.

Kaleel et al. [65] developed a new numerical framework for modeling progressive delamination in bilayer laminated materials using 1-dimensional component-based models with CUF. They emphasized that their proposed model achieves 3D-like accuracy with lower rendering costs, without aspect ratio constraints in complex structures, analysis times, and delamination. They used the binary constitutive law based on Mixed-mode delamination in this new numerical framework and stated that these high-order

adhesive elements mimic the structure-component adhesion mechanics in the structure [66].

In a detailed literature review, delamination and CZM analysis for FGM and layered composites are very important in damage detection. Many new approaches and models are still proposed in order for these analyses to yield accurate results. In this thesis, the CUF model was used together with CZM for the 1D delamination analysis of the 10-layer FGM cantilever beam, which was not previously included in the literature. Here, using CUF, the CZM is modeled as a FEM scheme. In this respect, our study is original and contributes to the literature.

1. CHAPTER

GENERAL INFORMATION AND LITERATURE STUDY

1.1. Problem Status

In this thesis, the CUF model is used together with CZM for 1D delamination analysis of a 10-layer FGM cantilever beam. Here, using CUF, the CZM is modeled as a FEM scheme. The beam consists of 10 layers, the first layer is 100% metal and the 10th layer is 100% ceramic. Among these materials, the ceramic one is Al2O3, the metal one is Ni, and its material properties are shown in Table 1. The material properties of the interlayers are graded on the basis of the Mori-Tanaka diagram and the equations given in Equation 1-7 are used in this grading. Forces (F=10 KN) are acting on this cantilever beam as shown in Figure 1 and delamination analysis will be performed to determine the openings and laminations that will occur here. The beam's height (h=0.4m), width (b=0.2m), and length (L= 10m) are shown (Fig. 1).

Table 1. Properties of ceramics (Al_2O_3) and metal (Ni)

Property	Ceramics	Metal
Elasticity Modulus E (GPa)	370	207
Shear Modulus G (GPa)	150	76
Bulk Modulus K (GPa)	172	180
Poisson Ratio (v)	0.22	0.31

The ceramic material used is Al2O3 and the metal material is Ni. Physical and mechanical properties of materials are given in Table 1 [69].

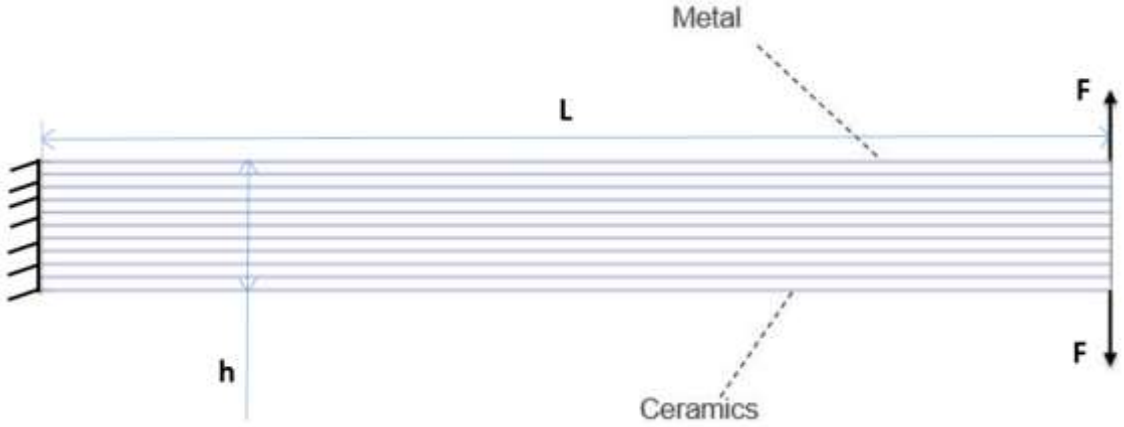

Figure 1. The geometry and forces positions of the problem analyzed in this thesis

1.2. Functionally Graded Materials

The material will be used is consisting of ten layers and to get the functionally grading behavior Mori-Tanaka scheme will be used. The Mori-Tanaka technique utilizes mean stress and strain fields within the composite's components to approximate the overall material characteristics of the composite. The Mori-Tanaka approach was proposed by Mori and Tanaka in 1973. It entails intricate manipulations of field variables involving concepts like eigenstrain and backstress [70].

The Mori-Tanaka scheme equations used in this thesis are given as follows [71]:

Volumetric ratios:

$$V_c = \left(\frac{z+\frac{h}{2}}{h}\right)^n \qquad when \quad z = \left[-\frac{h}{2}, \frac{h}{2}\right] \tag{1}$$

$$V_m = 1 - V_c \tag{2}$$

Bulk modulus:

$$K = K_m + \frac{V_c\,(K_c - K_m)}{1+(1-V_c)\frac{3(K_c-K_m)}{3K_m+4G_m)}} \tag{3}$$

Shear modulus:

$$G = G_m + \frac{V_c\,(G_c - G_m)}{1+(1-V_c)\frac{(G_c-G_m)}{G_m+f_1}} \tag{4}$$

$$f_1 = \frac{G_m(9K_m+8G_m)}{6(K_m+2G_m)} \tag{5}$$

Elasticity modulus:

$$E = \frac{9KG}{3K+G} \quad (6)$$

Poisson ratio:

$$v = \frac{3K-2G}{2(3K+G)} \quad (7)$$

Where the subscript c stands for ceramics and m stands for metal.

1.3. CZM (Cohesive Zone Model)

The basis of the cohesive zone modeling technique is based on the work of Dugdale and Barenblatt [30]. This technique is based on the progressive reduction of the strength of the bond between the two surfaces in the delamination zone, instead of completely disappearing when damaged. It is intensely preferred when delamination analysis of composites with finite elements is performed due to its ease in applications and the need for few parameters to be obtained through experiments. Therefore, many researchers use cohesive surface elements by numerically calculating the delamination in experimental studies.

Figure 2 shows the cohesive field elements in the finite element model. Cohesive field elements can be modeled as solid elements with no volume or with volume, or with two-dimensional four-node shell elements. The cohesive field elements placed on the surface where the layers forming the composite material come into contact with each other are defined by the pull-separation law. These elements open until the loss of tensile strength occurs and consume energy during this time. This region where the energy is spent is called the cohesive field. For this reason, in order to calculate the delamination in the damage analysis of composite structures, the fracture toughness between layers should be known. Fracture toughness is measured by the resistance of the material during delamination and is defined by the critical strain diffusion rate. It is necessary to perform some tests for the parameters of the cohesive field elements. These tests are the Double Cantilever Beam test; it is the test of choice for the experimental determination of interlayer mode I fracture toughness. This test is important because the strength of the material is learned under the influence of strain in the thickness direction. Three-pronged Notch Flexural Test; It is used to determine the mode II fracture toughness of systems that will be subjected to compression. Mixed Mode Bending test is; It is a test performed

by forcing the system to open and slide with the delamination test device located at the beginning of the system bending test under the influence of mixed mode (Mode I and Mode II).

The failure delamination modes in this section are related to the loads applied to the material, namely normal and shear effects. Figure 3 shows the delamination modes. Mode 1 is defined as opening (tensile) and the displacement of the crack surfaces is perpendicular to the crack surface. In Mode II, the displacement of the cracked surfaces is in the crack plane and is defined as shear loading. Mode III is defined as shear loading and the displacement of the crack surfaces is parallel to the crack surface. Apart from these, there is also Mixed Mode loading which is a combination of tensile, shear, and shear loads.

Parameters influencing the cohesive zone model:
The first parameter is the law of attraction in cohesive field modeling and it is the most important parameter. This law, elastic field, and plastic field determine the behavior of the cohesive element.

For example; When the trapezoidal law is chosen, it provides greater displacement and higher tensile loads than the exponential law. In addition, while some tensile laws give good results with ductile materials, some may be more suitable for brittle materials. Choosing the appropriate law is also important for the accuracy of the results.

The second parameter is the effect of maximum tensile load. This value is important in calculating the point at which the cohesive field element will be completely damaged and is expressed according to this value whether the adhesive element is brittle or ductile. As the maximum tensile load decreases, the critical clearance between the bonded surfaces increases.

The third parameter is the critical spacing between the adhesive surfaces and the critical energy diffusion rate, which is one of the other factors affecting the cohesive field model since it defines the stiffness and elastic region. The reduction in critical energy release

rate will also reduce the critical opening amount without a change in maximum tensile load. A high critical opening amount can be advantageous at fatigue loads.

The fourth parameter is the shear components of the critical energy release rate and the maximum tensile load. This situation is more related to mixed mode loading and how the related pull law calculates this situation. Some adhesive materials have better shear load properties while others have better tensile load properties. This is important in the emergence of different mixed-mode cohesive field models and deciding which damage will occur first.

The fifth parameter is the size of the selected cohesive elements when applying the cohesive field model technique with finite elements. When the finite elements used are too large, oscillations may occur in the force-displacement curve or the model may not be stable. Although reducing the element size eliminates this problem, the number of elements increases, and the computation time increases. Therefore, the optimum element size must be determined.

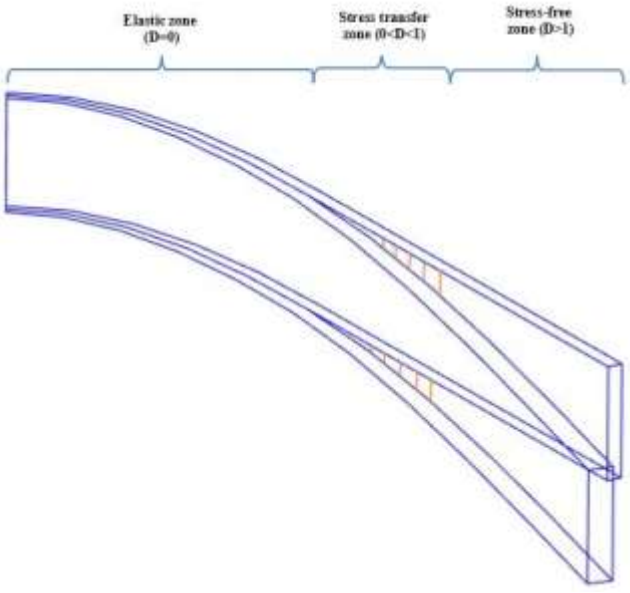

Figure 2. The modelling of cohesive zone

Traction-Separation Law

The tensile-split law is a version of the cohesive field law engineering stress-strain curve modified with stress and displacement parameters. It determines the basic behavior that

determines the relative displacement between two points and the resulting load. Traction laws appear in the literature in various forms: linear, non-linear, continuous, and discontinuous. Any traction law chosen determines the behavior of the two segments. The first part shows the area from the starting point to the point where the damage will begin to occur. This range can be expressed as the rigidity of the structure. The damage initiation point can be defined as the maximum tension T_{max} calculated according to the damage criteria and the known basic properties of the material, or the displacement at the moment of maximum tension δ_c (Figure 3).

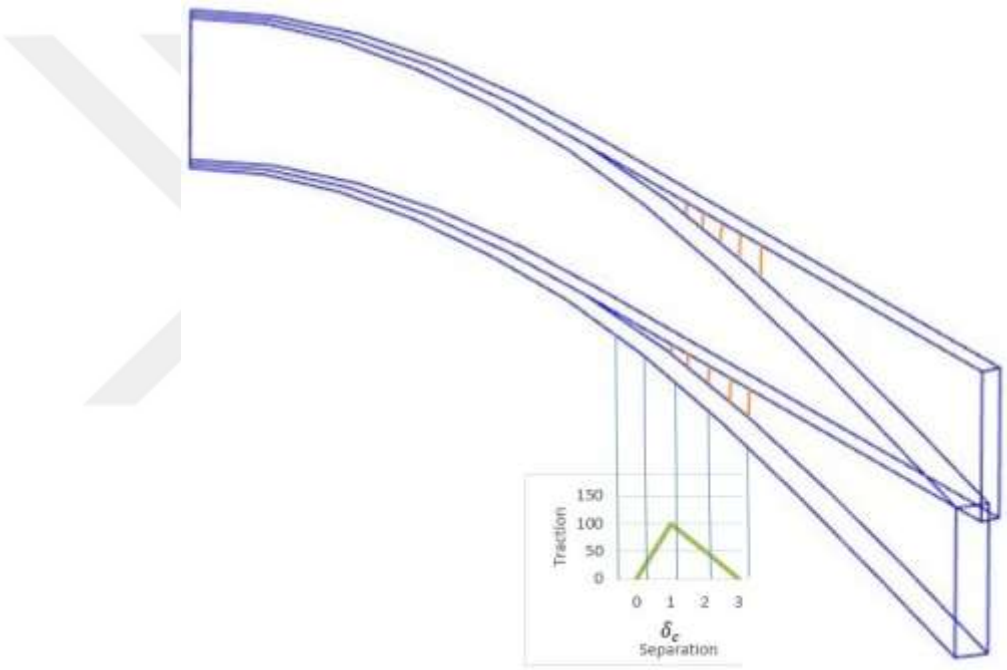

Figure 3. Traction-separation law

As shown in Figure 3 the damage starts when the separation reach a value of δ_c. Then damage causes decrease in the area bearing the load and smaller stress causes higher separation. Lastly the material separated totally with 3 unit in this example and it can no longer bear strass.

As the displacement continues to increase after the damage initiation point is reached, the initial elastic behavior is replaced by the behavior in the second part of the tensile law. This section represents the distance between the damage initiation point and the rupture point and is calculated with the damage progression criterion. The damage progression criterion is defined by the critical energy release rate Gc. The energy diffusion rate, often

called cohesive energy, is the area between the attraction law curve and the y-axis. When the critical energy diffusion rate value is reached, zero or very close to zero tensile value is obtained. At this stage, since the tensile value is zero and there is no force to hold the materials together, all the damage occurs, the relevant cohesive zone disappears and crack propagation occurs.

The most commonly used tensile laws in the literature and experimental studies are the bilinear law, trapezoid law, and exponential law.

Bilinear law; Bilinear or triangular tensile law is triangular as shown in Figure 9 and the function is continuous and piecewise linear. Once the damage has started, the strength of the adhesive material is reduced linearly (Figure 4). It is generally preferred for crispy materials.

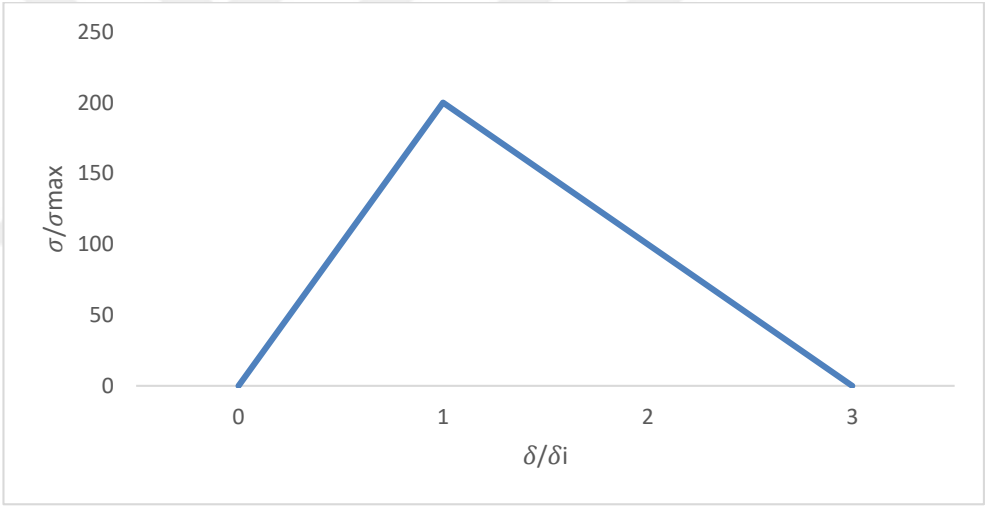

Figure 4. Bilinear traction-separation law

Trapezoid law; the technique presented by Tvergaard and Hutchinson is frequently preferred for ductile adhesive materials. It is a continuous and piecewise linear function (Figure 5).

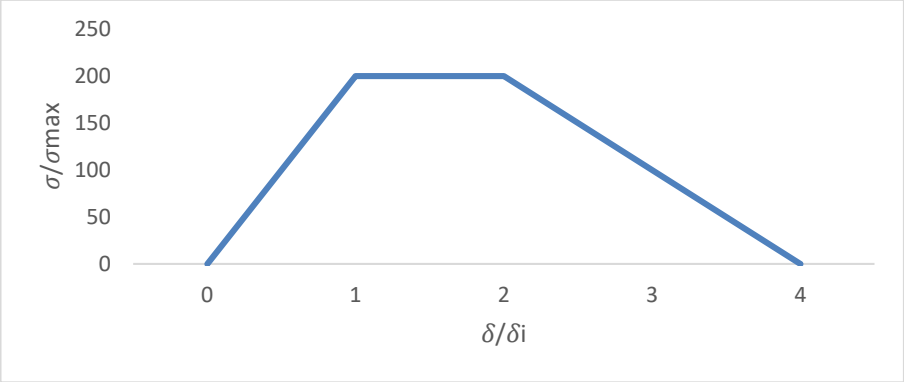

Figure 5. Trapezoid traction-separation law

Although the exponential law is difficult to calculate compared to other laws, it gives realistic results (the technique first presented by Xu and Needleman [67] is generally used in simple sample tests such as the DCB test (Figure 6)).

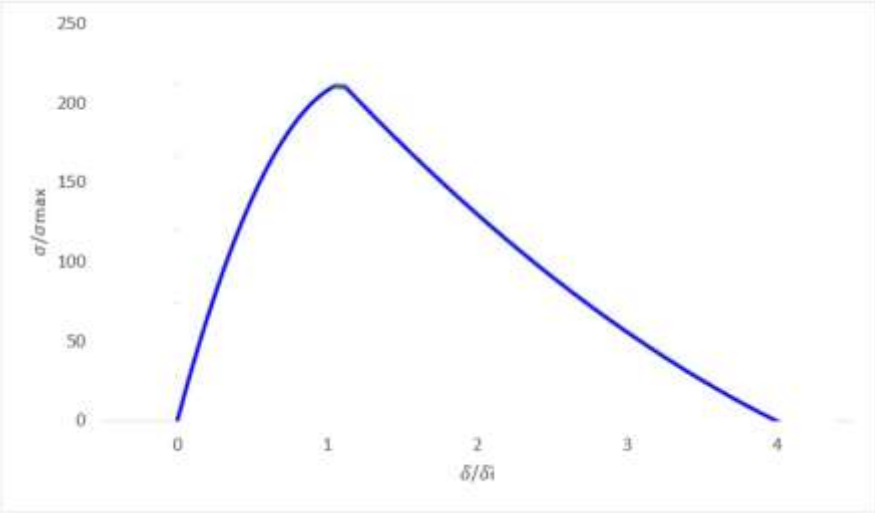

Figure 6. Exponential traction-separation law

1.4. Carrera Unified Formulation

The Carrera Unified Formulation (CUF) is a remarkable mathematical and computational framework employed in structural mechanics, particularly for the analysis of diverse composite structures. Crafted by Italian aerospace engineer Erasmo Carrera and collaborators, CUF stands out for its remarkable versatility in handling a wide spectrum of structures such as beams, plates, and shells, encompassing an extensive range of material properties and geometries. Its defining characteristic lies in its unified approach,

offering a consistent mathematical formulation irrespective of the structure's geometry or material properties. CUF accommodates higher-order theories, utilizing polynomial expansions for displacements, strains, and stresses, allowing precise representation of complex structural responses. It integrates a generalized one-dimensional theory that includes classical and advanced one-dimensional theories, enabling tailored analyses based on the problem at hand. Particularly notable is its adeptness in dealing with functionally graded materials (FGMs), making it invaluable for modeling FGMs and analyzing their mechanical behavior. By adeptly amalgamating mathematical tools like the Principle of Virtual Displacements (PVD) and Hamilton's principle, CUF derives governing equations and boundary conditions for the structure in question. Despite its sophistication, it maintains computational efficiency, rendering it practical for intricate structural analyses and optimizations. CUF finds extensive application in the analysis and design of composite structures, notably in the aerospace, automotive, and marine domains, where it accurately predicts structural response, deformation, and failure modes of composite materials and structures. In essence, Carrera Unified Formulation stands as a potent and adaptable framework, seamlessly bridging diverse theories and facilitating precise analysis across a broad spectrum of structures [68].

$$\boldsymbol{u} = N_i \boldsymbol{u}_i \tag{8}$$

$$\delta\boldsymbol{u} = N_j \delta\boldsymbol{u}_j \tag{9}$$

$$\boldsymbol{\varepsilon} = \boldsymbol{b}\boldsymbol{u} = \boldsymbol{b}N_i\boldsymbol{u}_i = \boldsymbol{B}_i\boldsymbol{u}_i \tag{10}$$

$$\delta\boldsymbol{\varepsilon} = \boldsymbol{b}\delta\boldsymbol{u} = \boldsymbol{b}N_j\delta\boldsymbol{u}_j = \boldsymbol{B}_j\delta\boldsymbol{u}_j \tag{11}$$

$$\boldsymbol{B}_i = \begin{bmatrix} N_{i,x} & 0 & 0 \\ 0 & N_{i,y} & 0 \\ 0 & 0 & N_{i,z} \\ N_{i,z} & 0 & N_{i,x} \\ 0 & N_{i,z} & N_{i,y} \\ N_{i,y} & N_{i,x} & 0 \end{bmatrix} \tag{12}$$

$$\delta L_{int} = \delta\boldsymbol{u}_j^T \left(\int_V \boldsymbol{B}_j^T \boldsymbol{C}\boldsymbol{B}_i dV \right) \boldsymbol{u}_i \tag{13}$$

$$\boldsymbol{k}^{ij} = \int_V \boldsymbol{B}_j^T \boldsymbol{C}\boldsymbol{B}_i dV \tag{14}$$

$$\boldsymbol{k}^{ij} = \begin{bmatrix} k_{xx}^{ij} & k_{xy}^{ij} & k_{xz}^{ij} \\ k_{yx}^{ij} & k_{yy}^{ij} & k_{yz}^{ij} \\ k_{zx}^{ij} & k_{zy}^{ij} & k_{zz}^{ij} \end{bmatrix} \quad \text{Fundamental Nucleus} \tag{15}$$

u: Displacement

N: Shape function

ε: Strain

b: Differential operator

B: Differential operator including shape functions

K: Stiffness matrix element

For 1D FEM Formulation $\rightarrow \delta L_i = \delta \boldsymbol{u}_{sj} \boldsymbol{k}^{\tau sij} \boldsymbol{u}_{\tau i}$

$$\begin{aligned} \boldsymbol{u} &= N_i(y) F_\tau(x,z) \boldsymbol{u}_{\tau i} \\ \delta \boldsymbol{u} &= N_j(y) F_s(x,z) \delta \boldsymbol{u}_{sj} \end{aligned} \tag{16}$$

as F is the section function that cause the variance over the section in 1d problems [68].

$$\begin{aligned} k_{xx}^{\tau sij} = \; & (\lambda + 2G) \int_l N_i N_j dy \int_A F_{\tau,x} F_{s,x} dA \\ & + G \int_l N_i N_j dy \int_A F_{\tau,z} F_{s,z} dA + G \int_l N_{i,y} N_{j,y} dy \int_A F_\tau F_s dA; \end{aligned} \tag{17}$$

$$k_{xy}^{\tau sij} = \lambda \int_l N_{i,y} N_j dy \int_A F_\tau F_{s,x} dA + G \int_l N_i N_{j,y} dy \int_A F_{\tau,x} F_s dA \tag{18}$$

For the Timoshenko beam those equations are applied through Tailor expansion

$$\begin{aligned} u_x(x,y,z) &= u_{x_1}(y) \\ u_y(x,y,z) &= u_{y_1}(y) + \phi_z(y) x + \phi_x(y) z \\ u_z(x,y,z) &= u_{z_1}(y) \end{aligned} \tag{19}$$

So by applying CUF for Timoshenko we need to accept $F_1 = 1$ $F_2 = x$ and $F_3 = z$. Also, the u_{y2}, u_{y3}, u_{z2} and u_{z3} must be panelized. Then, u_{y2} is considered as ϕ_z and u_{z2} as ϕ_x.

ϕ_z : Rotation around z axis

ϕ_x: Rotation around x axis

Now, to analyze delamination and discontinuities Lagrange expansion will be used to benefit from its properties in simulating discontinuities. Lagrange expansion have the section functions as shape function that approximate the property value on any point of the section by interpolating its values on the nodes.

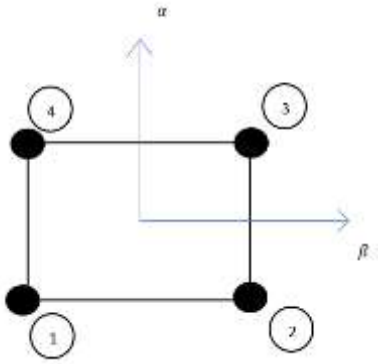

Figure 7. Four node Lagrange (L4) element in normalized geometry

Figure 7 shows the Lagrange L4 element as in the normalized geometry. In both directions the sides have standard 2 units long. Knowing the coordinates of each node, section functions F will be the shape functions of 2D 4 node surface and can be calculated as follows:

$$F_\tau = \frac{1}{4}(1 + \alpha\alpha_\tau)(1 + \beta\beta_\tau), \tau = 1,2,3,4 \qquad (20)$$

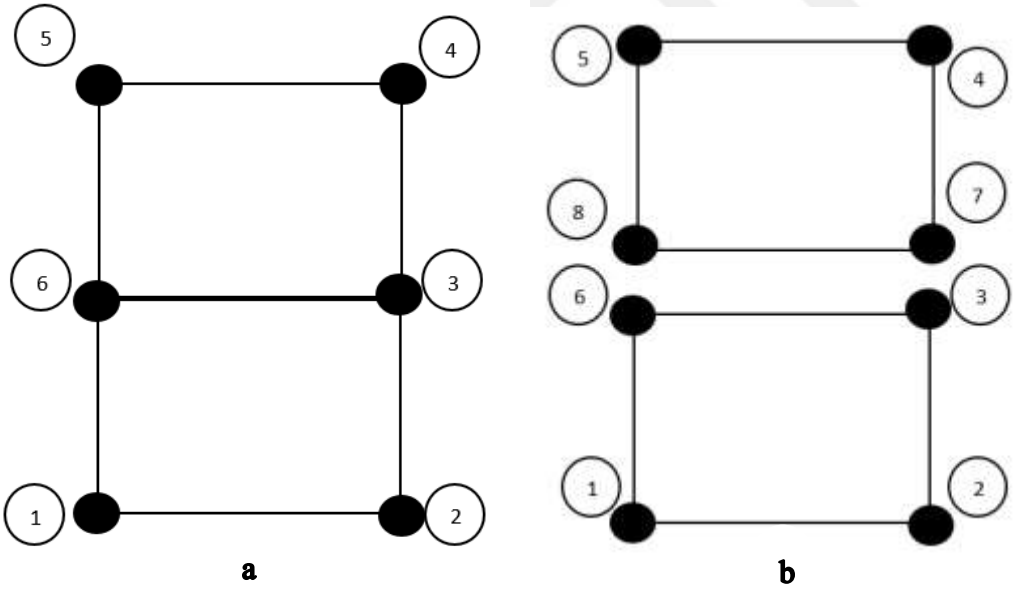

Figure 8. 2 Lagrange elements (2L4) to model a beam of 2 layers. a) In case of no crack. b) In case of existing crack.

The advantage of using Lagrange elements that let us applying it in our study is the ability to describe discontinuities in easy and practical way. This can be seen in Figure 8.

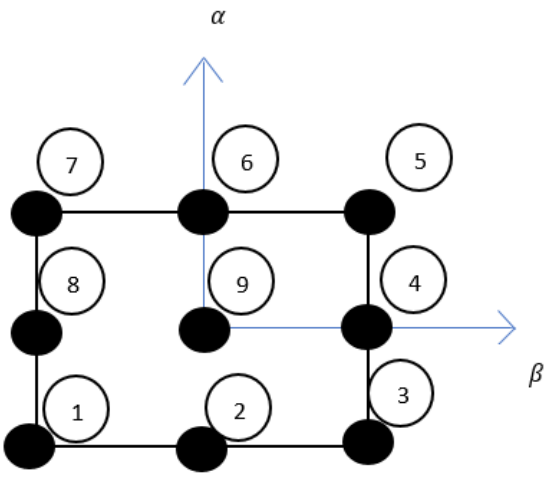

Figure 9. Nine node Lagrange (L9) element in normalized geometry.

When using the nine node Lagrange elements (L9) the section functions on each node will be the shape functions used for 2d surfaces with similar nine node distribution. Those are described in the following equations:

$$F_\tau = \frac{1}{4}(\alpha^2 + \alpha\alpha_\tau)(\beta^2 + \beta\beta_\tau)\ , \tau = 1,3,5,7$$
$$F_\tau = \frac{1}{2}\beta_\tau^2(\beta^2 + \beta\beta_\tau)(1-\alpha^2) + \frac{1}{2}\alpha_\tau^2(\alpha^2 + \alpha\alpha_\tau)(1-\beta^2)\ , \tau = 2,4,6,8 \qquad (21)$$
$$F_\tau = (1-\alpha^2)(1-\beta^2)\ , \tau = 9$$

The 2-layer cracked beam analysis with L9 elements are also done with the same logic used for L4 elements explained in Figure 8.

Exploiting Lagrange elements in 1D CUF analyses gives us a 3D like precision with relatively very low computational cost.

1.5. Applying Cohesive Zone Model (CZM) To Carrera Unified Formulation (CUF)

Lagrange elements explained in the previous section made it possible to apply CZM. The 2L4 elements shown previously in Figure 8-b are edited by additional 2 springs between nodes 3-7 and 6-8. When the springs are given a relative very high stiffness value the elements become equivalent to the crack-free 2L4 element shown in Figure 8-a. In case of the cohesive zone existing between 2 layers as in our problem, the springs will be

acting according to the traction-separation law. The settlement of the springs on the 2L4 elements is shown in Figure 10.

Lagrange elements are unique with their node number adjustability. Every node can be divided to two different nodes when required. Instead of the elements are sharing a node they will have two different nodes with a spring between then representing the cohesive effect.

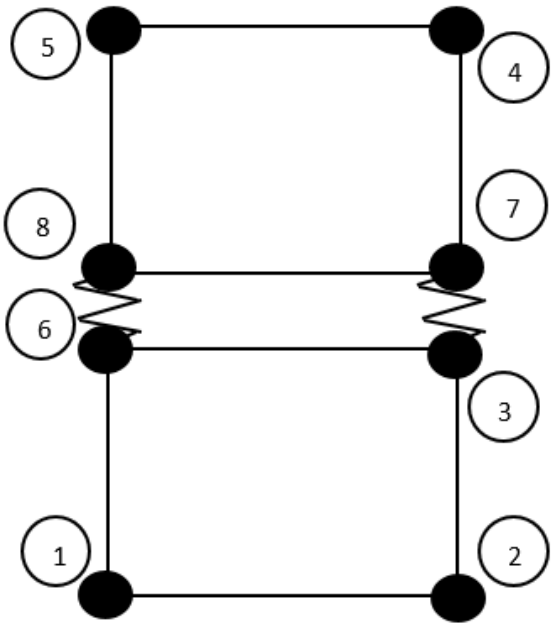

Figure 10. Applying CZM to CUF 2L4 Lagrange elements by adding 2 spring

In our analysis the bilinear traction separation law in Figure 4 will be used.

The parameters in the cohesive zone model are usually taken from experimental tests. In this thesis the values are determined arbitrarily as follows:

The separation when the damage is occurring is assumed to be

$\delta_{failure} = 1\ mm = 0.001\ m$

Maximum stress (traction):

$\sigma_{max} = 5 * 10^6$ MPa

K_n is stiffness taken from the traction separation law. It is the current traction value divided by current separation value (in the first part of the bilinear traction separation law):

$K_n = 2 * 10^9$ Mpa/m

After entering those values of the traction separation law the following calculations are to be made:

The area per node:

$A_{node} = \frac{b}{2} . \frac{L_{element}}{2}$ when b is the width of the section (22)

Stiffness of the spring K_s to be added to global stiffness matrix can be calculated by the force /separation value instead of the previous stress (traction)/ separation value for K_n :

$K_s = K_n . A_{node}$ (23)

The initial separation that cause maximum stress and represent the point of starting damage:

$\delta_{initial} = \frac{\sigma_{max}}{K_n}$ (24)

The force in the spring that cause maximum stress and represent the point of starting damage:

$F_{smax} = \sigma_{max} . A_{node}$ (25)

The total separation that full damage:

$\delta_{total} = \delta_{initial} + \delta_{failure}$ (26)

For refreshing the values and applying the traction separation law:

The separation is calculated as the difference of the displacements for the 2 nodes bonded by a spring.

Stress in the spring value is refreshed when $\delta_{initial} < \delta < \delta_{total}$:

$$\sigma = (\delta_{total} - \delta) * \frac{\sigma_{max}}{\delta_{failure}} \quad (27)$$

Then the spring contribution to the global stiffness matrix is also recalculated:

$K_s = \frac{\sigma A_{node}}{\delta}$ (28)

When $\delta > \delta_{total}$ the spring contribution to the global stiffness matrix become 0.

The code will keep refreshing separation values and calculating the corresponding stress values of the spring according to traction separation law. Then the spring stiffness will be calculated and its contribution will be adjusted. This process will be done in parallel with

increasing the force applied. After the force is applied totally the code will also keep refreshing separation to continue showing the dynamic simulation.

1.6. Purpose of the research

It is important to understand the complex damage mode of delamination of FG structures and laminated composites. Researchers want to find the causes of delamination by estimating the onset and spread of delamination by experimental or numerical methods. Thus, they can form composite materials that are resistant to delamination.

Numerical calculations can be made using fracture mechanics and damage mechanics approaches to determine delamination. When nonlinear material properties are neglected, successful results are obtained with Linear elastic fracture mechanics (LEFM) in delamination calculations. In addition, there are VCCT (Virtual Crack Closure Technique), J-integral, and VCET (Virtual Crack Extension Technique) techniques based on the fracture mechanics approach. For VCCT and J-integral, crack initiation and direction must be specified at the beginning. In the delamination calculations using the damage mechanics approach, CZM is created in the region where the delamination will occur in the models and the stress and displacement calculations are made by using the stiffness of the cohesive region in the elements in this area. When the determined limit values of the material are reached, the beginning of damage is seen and when the fracture toughness is reached, rupture occurs. In this way, the layers begin to separate from each other, new crack areas are formed and delamination growth occurs. In the cohesive field model technique, the crack can occur in any region and in any direction where the cohesive field elements are placed. It is also a more capable technique since it is easy to model ductile and brittle surfaces and integrate them into finite elements.

Our research aims to use the CZM to benefit from its multiple advantages by applying it in the FEM based CUF. Choosing CUF is to decrease the computational cost and to give a 3D like accuracy even while using 1D formulation. This is to the section functions that makes the variation possible in the section. The planned to be produced theory will also enjoy the easy refinement process of CUF when needed.

1.7. Importance of the Research

FGMs play an important role in different sections such as aerospace and industry. For example, there are many engineering applications being researched regarding FGM structures in industry. In particular, it is used for engine, suspension, and chassis components in the automotive industry, increasing fuel efficiency and driving experience. Additionally, FGMs improve safety by absorbing and dissipating energy during accidents. FGMs also reduce noise and vibration. FGMs' thermal and mechanical qualities make pistons, cylinder heads, and connecting rods more durable. They improve brake performance and reduce wear. This makes braking safer and more reliable. In the aerospace sector, FGMs is important for various critical components. FGMs provide strong thermal stability and mechanical stress resistance for gas turbine engine parts such turbine blades, vanes, and shrouds. This improves durability and reliability, making aircraft engines safer and more efficient. Besides strengthening wings, and tail components, it reduces the weight and improve the performance.

Aircraft wings, body sections, and composite panels experience variable mechanical loads, temperature changes, and environmental conditions during flight. These can start and spread delamination and make the structure weak. Delamination lowers component load-carrying capacity and increase fatigue probability. Undetected or poorly repaired delamination can cause unexpected failures.

Thus, engineers can evaluate failure criticality and take precautions by using numerical methods such as CZM for delamination analysis. Numerical methods may be very expensive for these complicated structures. In this thesis, using CZM integrated to CUF helps to decrease the computational cost while producing precise results.

2. CHAPTER

METHOD AND MATERIAL

My thesis used the CUF, CZM to model the delamination of FG beam. CUF and CZM were used together to perform delamination analysis of the 1-dimensional beam (Figure 1), consisting of 10 layers, with the bottom layer being ceramic and the top layer being metal. CZM was created based on the triangular traction-separatıon law.

CUF modeled and analyzed composite structures numerically. Lagrange elements were used (10 L4-elements in every section). Axially the quadratics shape functions were adopted as it saves computational power when compared to linear axial shape functions as will be shown in this chapter. CUF allows me to manage beams, laminates, and diverse loading circumstances and material attributes. Its unified nature let me effortlessly swap between displacement fields for accurate simulations with less processing effort than finite element methods. Also, CUF make it easy to model discontinuities.

CZM was essential for simulating delamination initiation and progression. Delamination was modeled accurately by formulating cohesive laws for interface mechanical response. This is because the failure is guided by the cohesive zone and that is what needed when the crack is to occur between layers and the crack propagation probability in the layer is not considered. Taking these advantages of CUF and CZM into consideration, it is predicted that CUF-CZM method to be used to analyze delamination in FGM provides a strong and efficient framework.

2.1. Results of Numerical Analyses

2.1.1 Taylor expansion (CUF)

In the beginning we used CUF with Taylor expansion. Linear shape functions were utilized and show the results for different number of elements.

The beam is 10-meter-long and his edge is subjected to -10000 N forces on the vertical axes.

For CUF in 1D we use the shape function in the axial direction N(y) and section function over the section F(x,z) as shown in equations (29-30).

The displacement and the virtual displacements are calculated according to:

$$\boldsymbol{u} = N_i(y)F_\tau(x,z)\boldsymbol{u}_{\tau i} \tag{29}$$

$$\delta\boldsymbol{u} = N_j(y)F_s(x,z)\delta\boldsymbol{u}_{sj} \tag{30}$$

For Timoshenko analysis by CUF the used displacement equations are as following:

$$\begin{aligned} u_x &= u_{x1} \\ u_y &= u_{y1} + xu_{y2} + z\,u_{y3} \\ u_z &= u_{z1} \end{aligned} \tag{31}$$

Now we start applying CUF to the bending problem with one vertical force before stepping to the delamination part and the CZM.

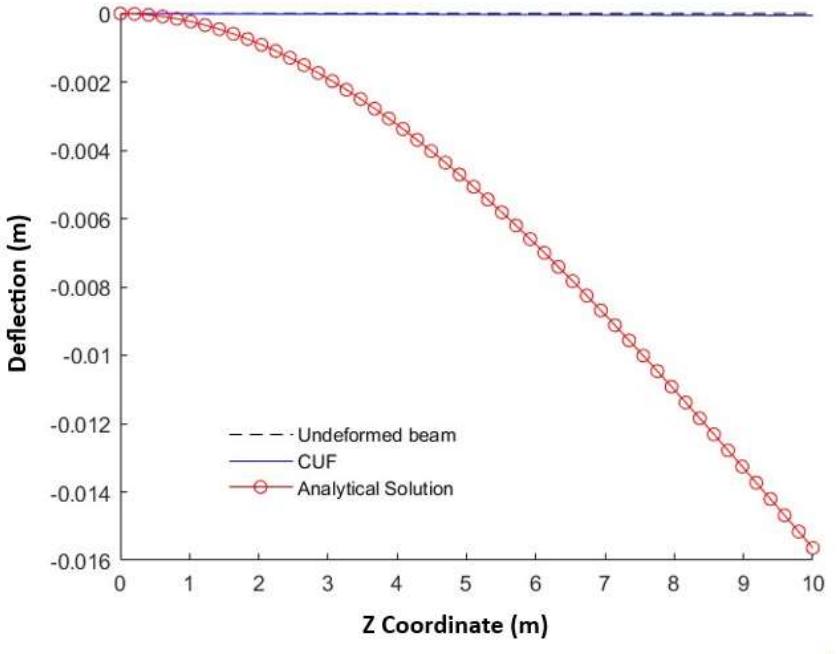

Figure 11. A comparison between a deformed Timoshenko beam modeled with CUF Taylor expansion discretized with one linear element and a deformed Timoshenko beam analyzed analytically.

In Figure 11, a comparison between the analytical solution of a Timoshenko beam and the resulted behavior of a Timoshenko beam analyzed by CUF and discretized to one element with Taylor expansion. The 1 element gave no significant displacement. The elements number will be increased in the following analyses to show correct results.

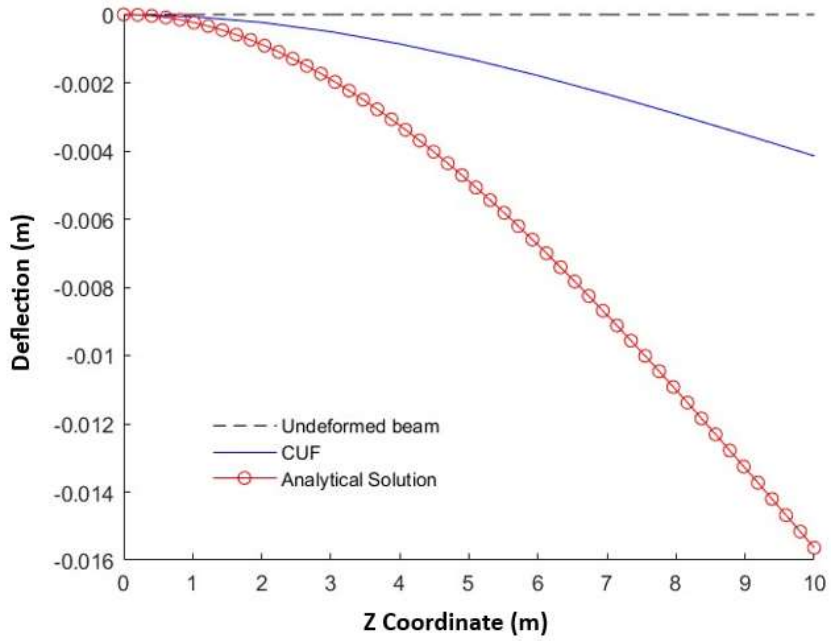

Figure 12. A comparison between a deformed Timoshenko beam analyzed by CUF (Taylor expansion) discretized with 10 linear elements and a deformed beam analyzed analytically.

After increasing the number of elements to 10,30,50,100, the results changed to gradually approach the analytical solution as shown in Figures 12,13,14 and 15 respectively. This shows that the analytical solution agrees with the formulation used by CUF applying Taylor expansion to model the Timoshenko beam bending problem.

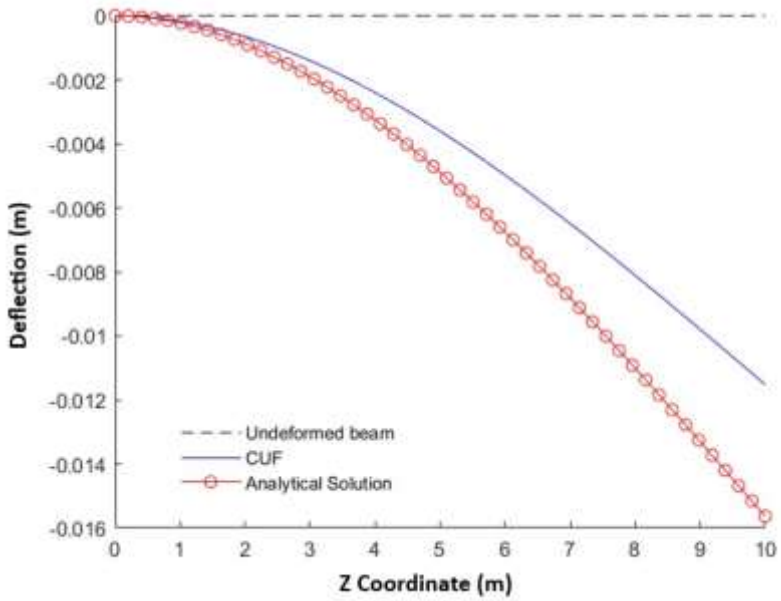

Figure 13. A comparison between a deformed Timoshenko beam analyzed by CUF (Taylor expansion) discretized with 30 linear elements and a deformed beam analyzed analytically.

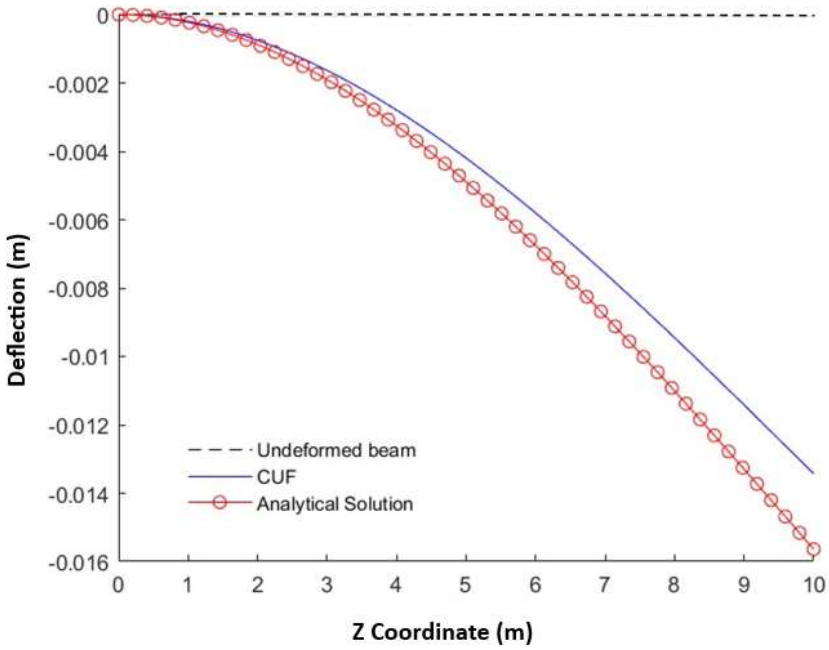

Figure 14. A comparison between a deformed Timoshenko beam analyzed by CUF (Taylor expansion) discretized with 50 linear elements and a deformed beam analyzed analytically.

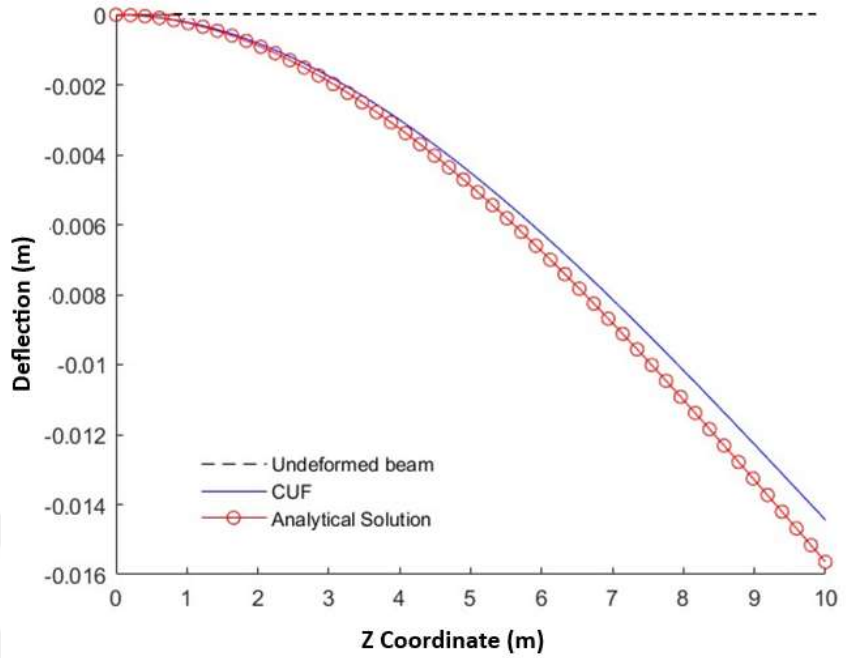

Figure 15. A comparison between a deformed Timoshenko beam analyzed by CUF (Taylor expansion) discretized with 100 linear elements and a deformed beam analyzed analytically.

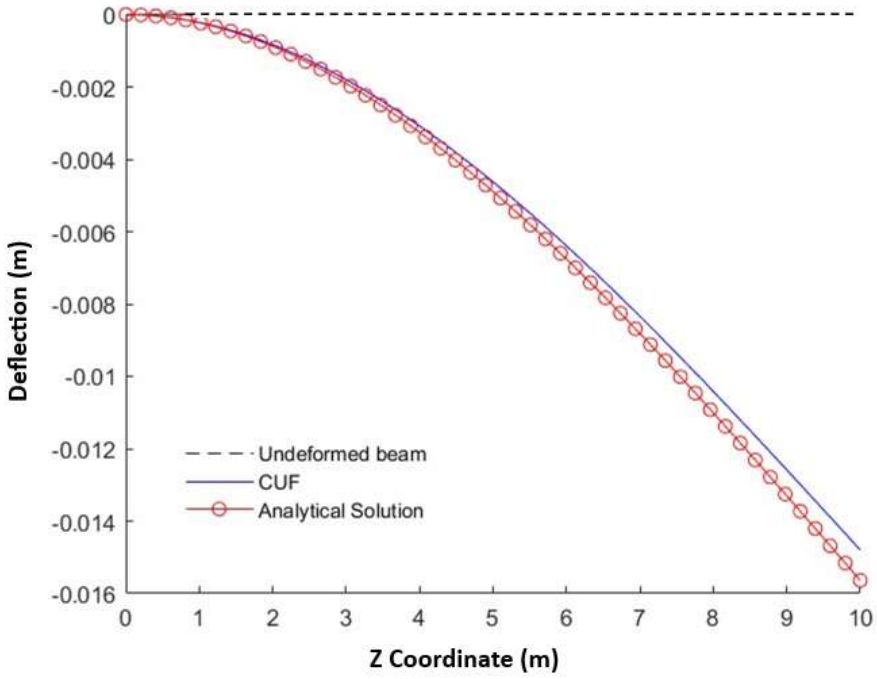

Figure 16. A comparison between a deformed Timoshenko beam analyzed by CUF (Taylor expansion) discretized with 500 linear elements and a deformed beam analyzed analytically.

In Figures 16 and 17 the comparison is made between the analytical solution of the Timoshenko beam and the result of Timoshenko beam analyzed with 500 and 1000 linear elements using CUF Tailor expansion respectively. After 500 elements refinement is not giving relevant improvement.

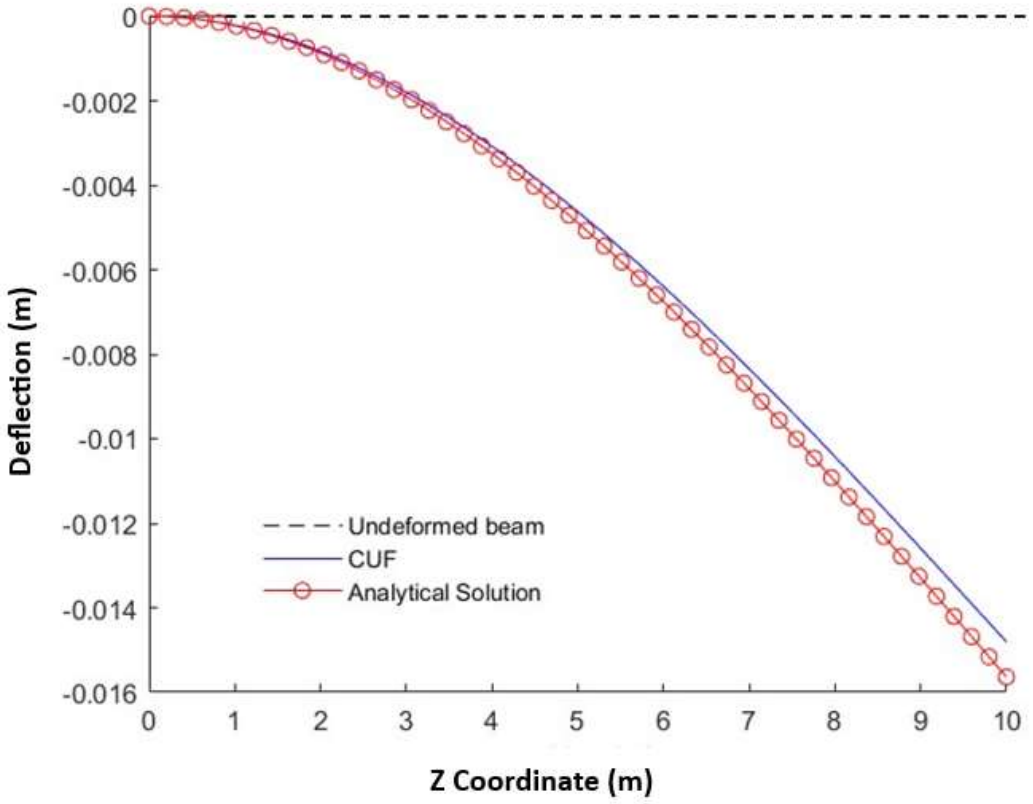

Figure 17. A comparison between a deformed Timoshenko beam analyzed by CUF (Taylor expansion) discretized with 1000 linear elements and a deformed beam analyzed analytically.

In all previous analyses the shape functions used in the axial direction are linear. By using quadratic axial shape functions, CUF is applied again with Taylor expansion to model the Timoshenko beam and results are compared with the analytical solution.

Using three nodes on the axial direction instead of 2 gives us Timoshenko like approach of CUF with higher precision. In Figure 18, the beam used has 3 elements ((9-1)*5) degrees of freedom and it shows a very much better results compared with the analysis of Figure 12 when the beam had 10 linear elements ((10-1)*5) degrees of freedom. In other

words, using quadratic axial shape functions allow us to get more precise results with less computational cost.

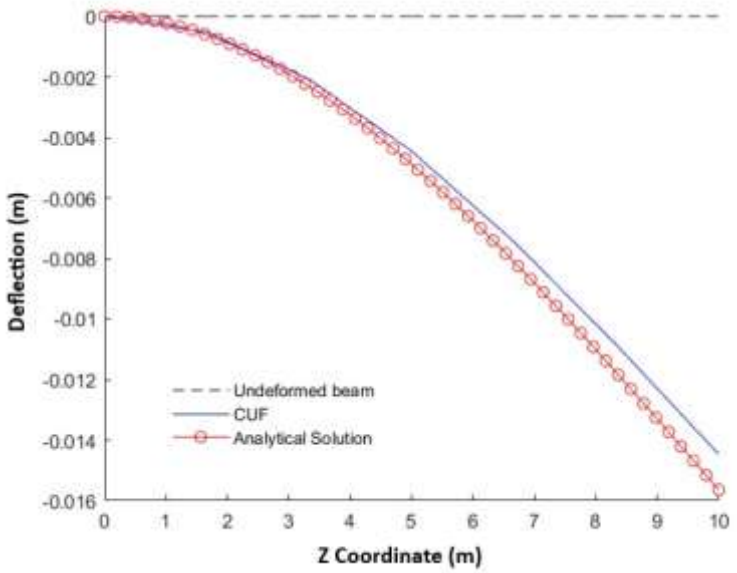

Figure 18. A comparison between a deformed Timoshenko beam analyzed by CUF (Taylor expansion) discretized with 3 quadratic elements and a deformed beam analyzed analytically.

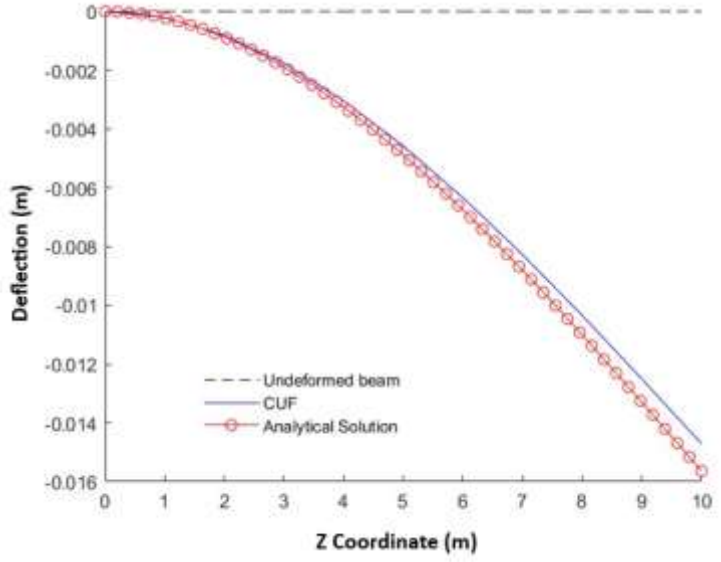

Figure 19. A comparison between a deformed Timoshenko beam analyzed by CUF (Taylor expansion) discretized with 5 quadratic elements and a deformed beam analyzed analytically.

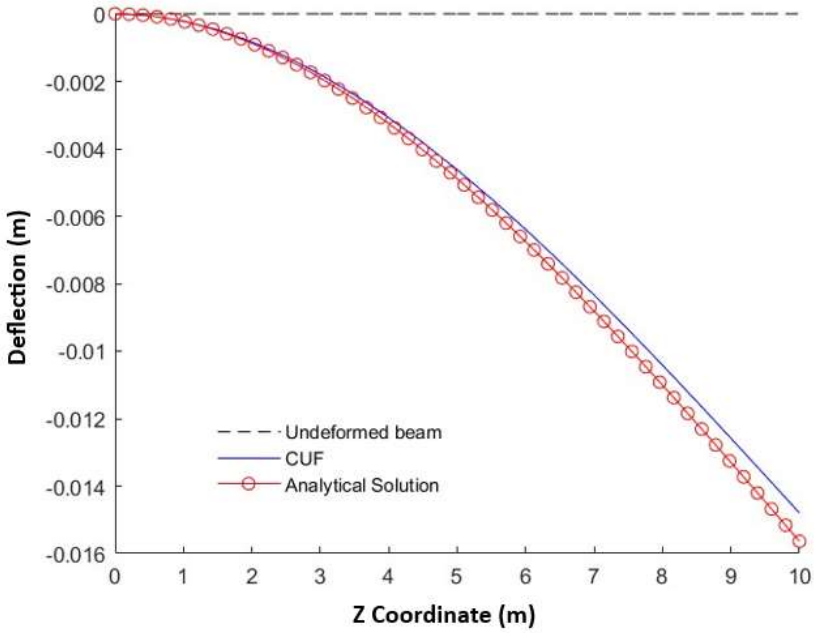

Figure 20. A comparison between a deformed Timoshenko beam analyzed by CUF (Taylor expansion) discretized with 10 quadratic elements and a deformed beam analyzed analytically.

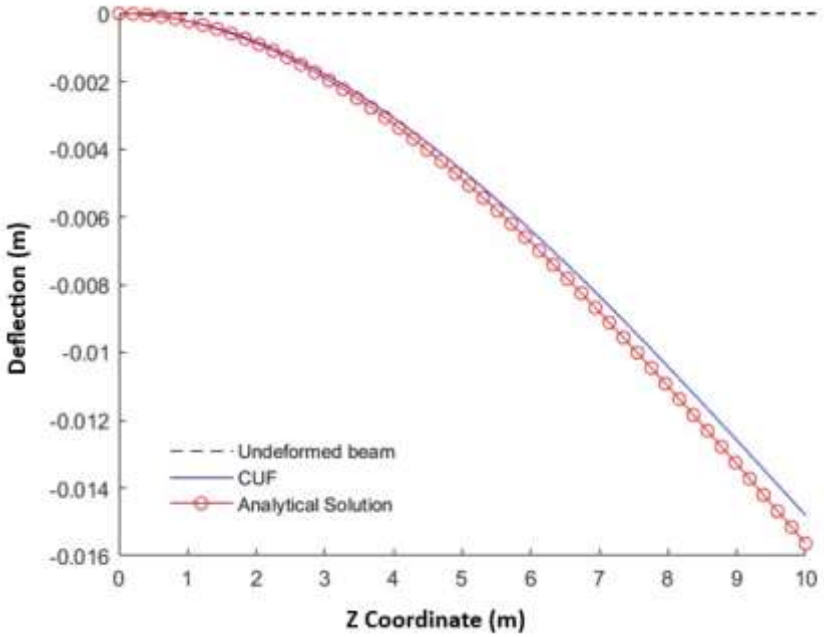

Figure 21. A comparison between a deformed Timoshenko beam analyzed by CUF (Taylor expansion) discretized with 100 quadratic elements and a deformed beam analyzed analytically.

In Figures 19,20 and 21 the analyses of Timoshenko like CUF beams with respectively 5,10 and 100 quadratic elements were shown compared to the Timoshenko beam analytical solution. It is noticeable that by using the quadratic shape functions, the effective refinement fell from 500 elements in the linear functions case to just 10 elements.

Now the Gauss numerical integration is used with linear shape functions.

With 100 elements the results as expected is the same as the results of exact integration (both with linear shape functions). Results are shown below in Figure 22.

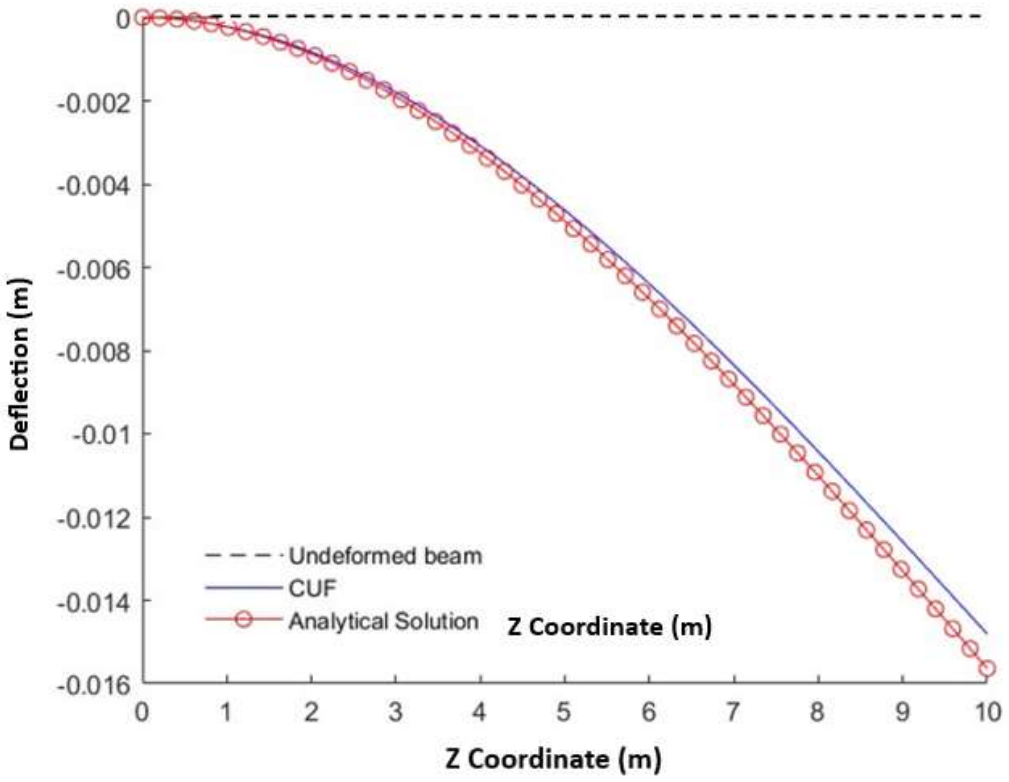

Figure 22. A comparison between a deformed Timoshenko beam analyzed by CUF (Taylor expansion) discretized with 100 linear elements using numerical integration and a deformed beam analyzed analytically.

2.1.2 Lagrange Expansion (CUF)

Now some results of the analyses I conducted using CUF with Lagrange Expansion will be shown. The problem taken is a structure of two layers with a crack in between layers at the end of the beam. A force is applied at the free end of the lower beam layer. I started modeling the section of this beam as 2 L4 elements and then tried 2 L9 elements. In both cases I employed linear and quadratic shape functions.

I also set the length of the crack to zero to check if the deflection result will agree with the one taken by the analytical solution. The results agreed with increasing the number of elements.

For this section we use equations 3 which explains CUF 1D equations for displacement and virtual displacement. However, the section function F will be expanded as the following so we get L4 Lagrange expansion:

$$F_m = \frac{1}{4}(1 + \alpha\alpha_m)(1 + \beta\beta_m) \qquad \alpha = 1,2,3,4 \qquad (32)$$

While α and β present the coordinates in the parametric space. α_m and β_m for m=1,2,3,4 show the coordinates of the related 4 edge points in the parametric space.

Later when we refer to L9 elements m will be a number between 1 and 9, 4 more points in the middle of the sides and one more point in the center of section will be added allowing a quadratic change across the section.

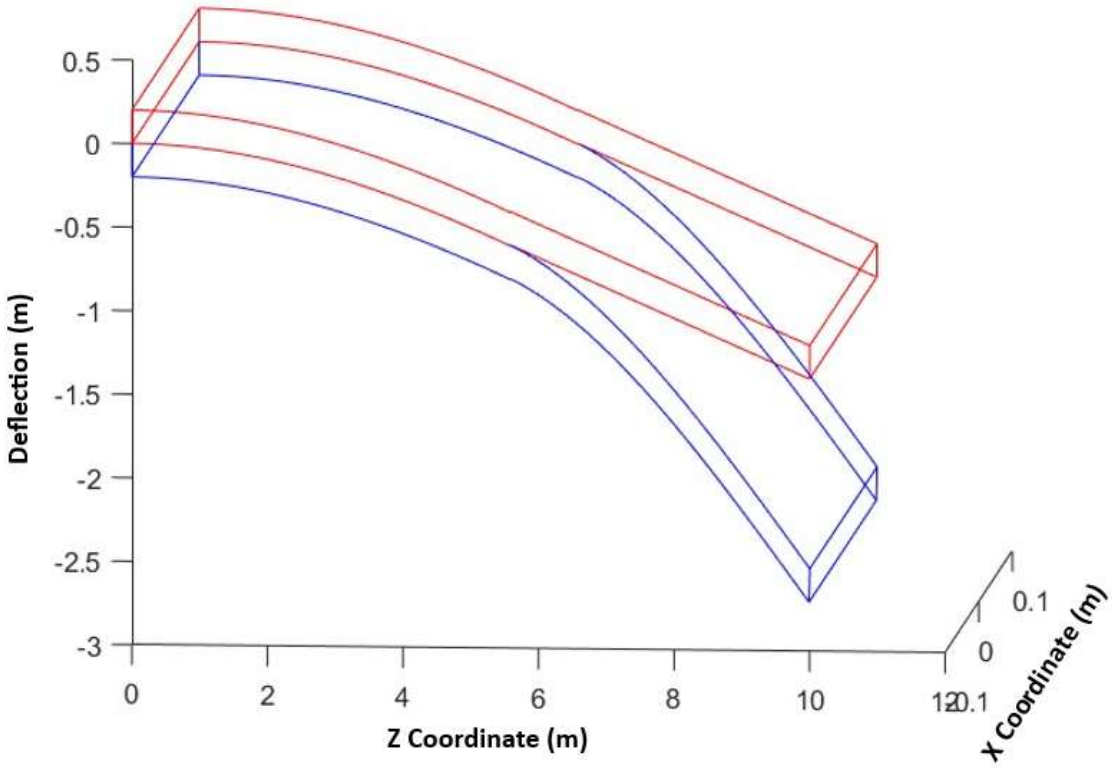

Figure 23. A 3D figure showing a deformed beam analyzed by CUF and discretized with 2L4 elements and quadratic axial functions.

One of the benefits of using Lagrange expansion is its ability to simulate discontinuities like cracks. This property can be noticed from Figure 23 which shows the deformed

cracked beam subjected to vertical force on its lower layer free end. This shows the capability of Lagrange elements of CUF to model discontinuities.

2.1.2.1 Crack-free beam

2.1.2.1.1 Using 2L4 elements and linear axial shape functions

In this part, 2L4 elements on the section will be used to discretize the beam with linear axial shape functions. The results with 100 and 200 elements are shown respectively in Figures 24 and 25. The validity of the scheme used was approved by comparing to analytical solutions for the bending problem. It is also seen that the accuracy increases proportionally with elements number.

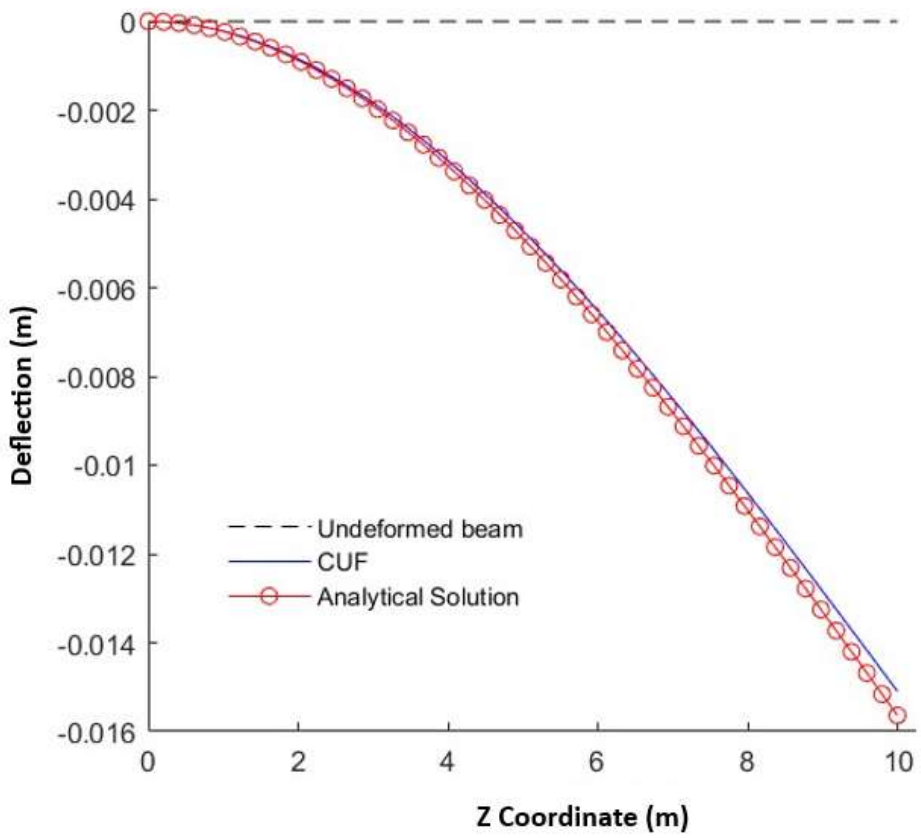

Figure 24. A comparison between a deformed beam analyzed by CUF and discretized with 100 2L4 elements using linear axial shape functions and a deformed beam analyzed analytically.

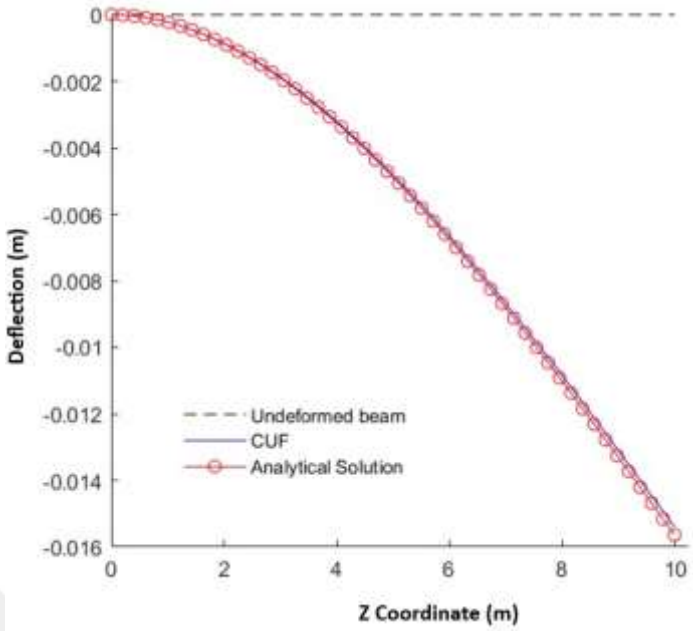

Figure 25. A comparison between a deformed beam analyzed by CUF and discretized with 200 2L4 elements using linear axial shape functions and a deformed beam analyzed analytically

2.1.2.1.2 Using 2L9 elements and quadratic axial shape functions

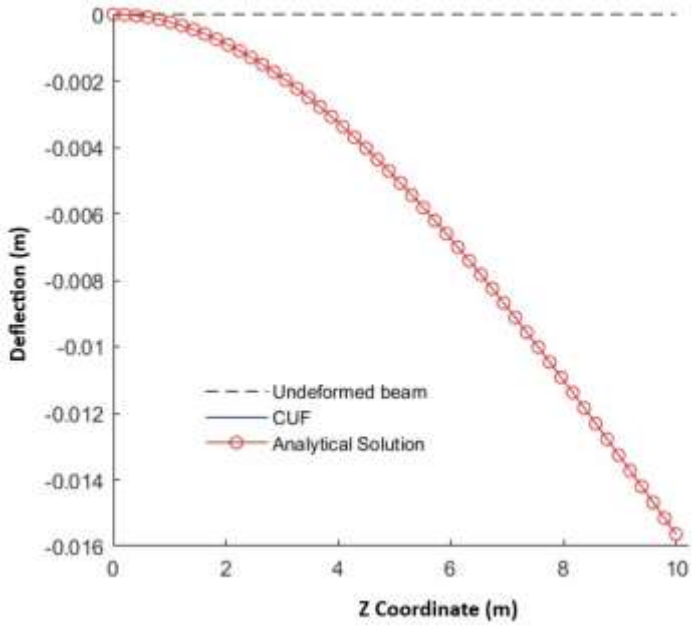

Figure 26. A comparison between a deformed beam analyzed by CUF and discretized with 50 2L9 elements using quadratic axial shape functions and a deformed beam analyzed analytically.

In Figure 26, 2L9 elements are used instead of 2L4 to permit quadratic change across the section. 50 elements are used. Also, the axial shape functions are set to be quadratic so there are nodes on 3 different sections on each element. The results show that using quadratic shape functions and 2L9 elements which are the quadratic equivalent to 2L4 elements helped to get much better results.

2.1.2.1.3 Using 2L4 elements and quadratic axial shape functions

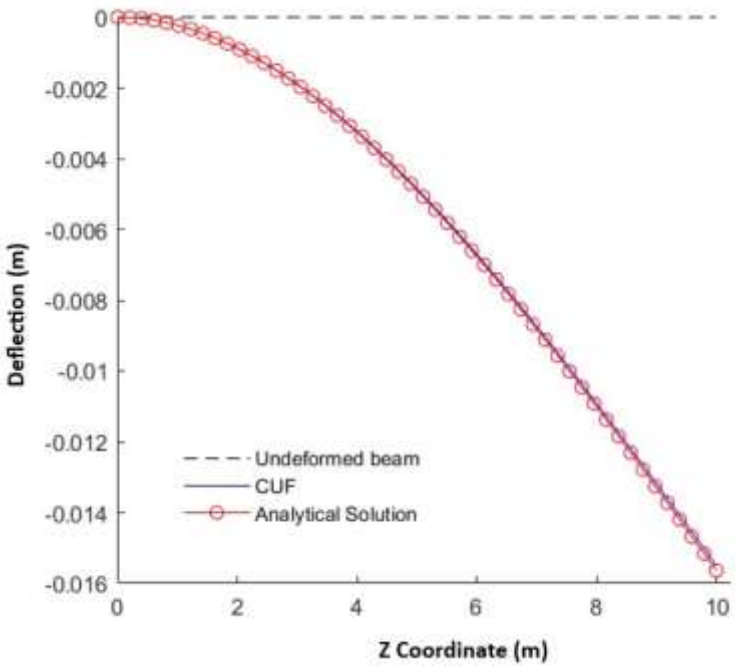

Figure 27. A comparison between a deformed beam analyzed by CUF and discretized with 50 2L4 elements using quadratic axial shape functions and a deformed beam analyzed analytically.

In Figure 27, 2L4 elements are used and quadratic axial shape functions. The number of elements is 50. Even with 2L4 elements instead of 2L9 elements, the results are still much better compared to the 2L4 elements with linear axial shape functions. we notice that the quadratic shape functions in the axial direction helped with decreasing the required degrees of freedom letting 50 elements give the same result of 200 elements with linear axial shape functions.

2.1.2.1.3 Using 2L9 elements and linear axial shape functions

In Figure 28, we see that the 2L9 elements couldn't give very precise results when used with the linear axial shape functions. This proves that the quadratic in plane shape functions (2L9) are not very efficient in this problem as they increase the degrees of freedom a lot and not affect the result at the same level in this deflection problem. Therefore, in our next analyses L4 elements will be used with quadratic axial shape functions.

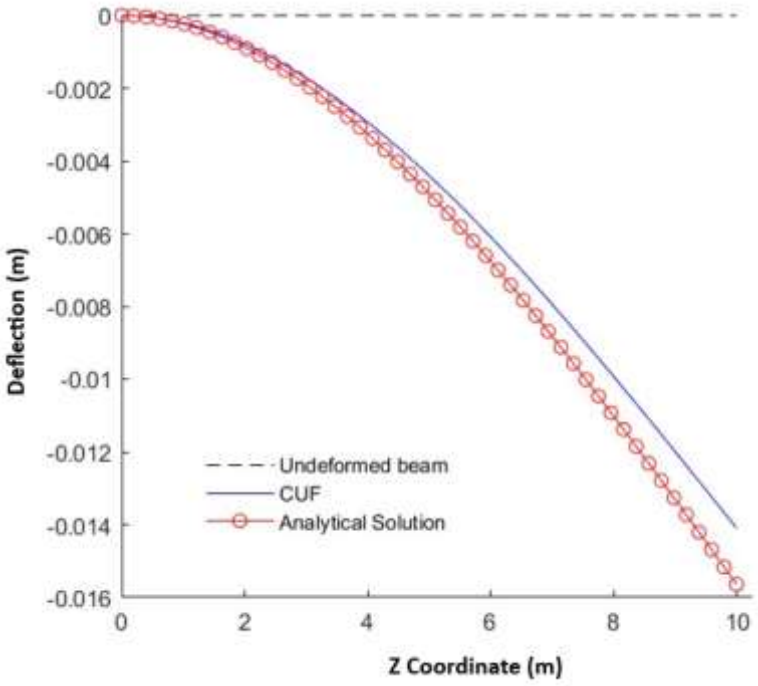

Figure 28. A comparison between a deformed beam analyzed by CUF and discretized with 50 2L9 elements using linear axial shape functions and a deformed beam analyzed analytically.

2.1.2.2 Cracked beam

Here in this section a cracked beam subjected to bending force will be analyzed. 2L4 elements with quadratic axial shape functions will be used. 50 2L4 elements will contain 6 nodes (2 nodes are common for each L4 element) on each section and the last 20 elements near to the free end will contain 8 nodes (no common nodes so there is a crack in the middle of the two L4 elements). The result of this analysis is shown in Figure 29

also compared to the analytical solution for the bending problem without considering the crack.

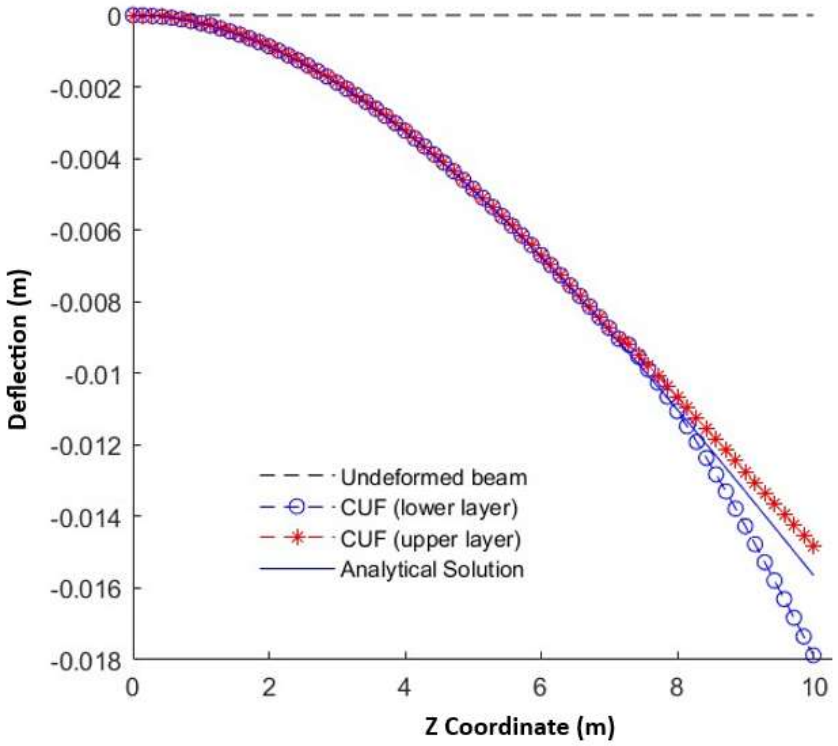

Figure 29. A comparison between a deformed beam analyzed by CUF and discretized with 50 crack-free /20 cracked 2L4 elements using quadratic axial shape functions and a deformed crack-free beam analyzed analytically.

2.2. CZM

The CZM is applied hear using CUF to simulate the crack propagation for the previous analyzed 2-layer beam. The beam has a crack between the 2 layers at the free end. Different from the previous problem two opposite forces are now applied to the upper and lower parts causing the crack to propagate. Each force is equal to 10000 N.

The code is refreshing the values of the cohesive zones elements values according to the Traction-Separation law shown. After the displacement reaches its maximum value the elements will be shown as red lines. In Figure 30, the 3D figure is showing the propagation of the cohesive zone. The red lines show cohesive elements that are not effective anymore (Totally damaged or $\delta > \delta_{Total}$).

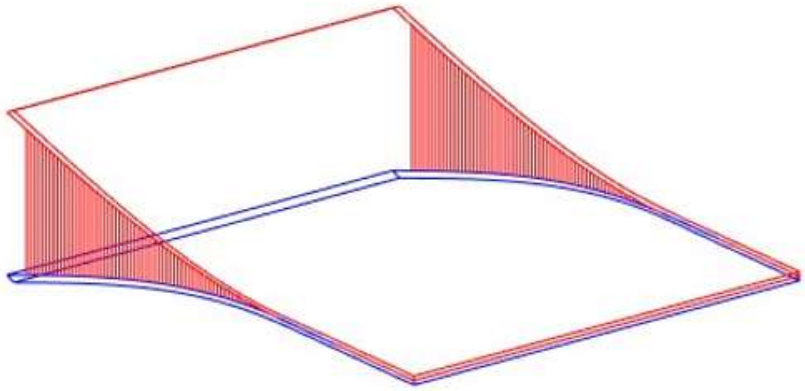

Figure 30. A 3D figure showing the propagation of the cohesive zone of a 2-layer beam delamination analysis conducted using CUF (Lagrange expansion) and CZM. The red lines show cohesive elements that are not effective anymore (Totally damaged).

2.3. FGM

My thesis used CUF, CZM to model delamination of FGM beams. CUF modeled and analyzed composite structures numerically. CUF allows me to manage beams, laminates, and diverse loading circumstances and material attributes. Its unified nature let me effortlessly swap between displacement fields for accurate simulations with less processing effort than finite element methods. Also, CUF make it easy to model discontinuities. CZM was essential for simulating delamination initiation and progression. Delamination was modeled accurately by formulating cohesive laws for interface mechanical response. CUF, CZM, and FGM provided a strong and efficient framework.

3. CHAPTER

RESULTS

3.1 Verification of The Numerical Model

After preparing the algorithm to solve the delamination problem of a FGM beam using CZM and CUF, the verification was made as a comparison with the analytical solution of the single material beam bending.

For this comparison to be meaningful, the two materials were held the same so the beam became also of single material. Moreover, the degrees of freedom between the layers were canceled by the penalty method. In other words, the stiffness of the cohesive zone was highly increased compared with other stiffness matrix values.

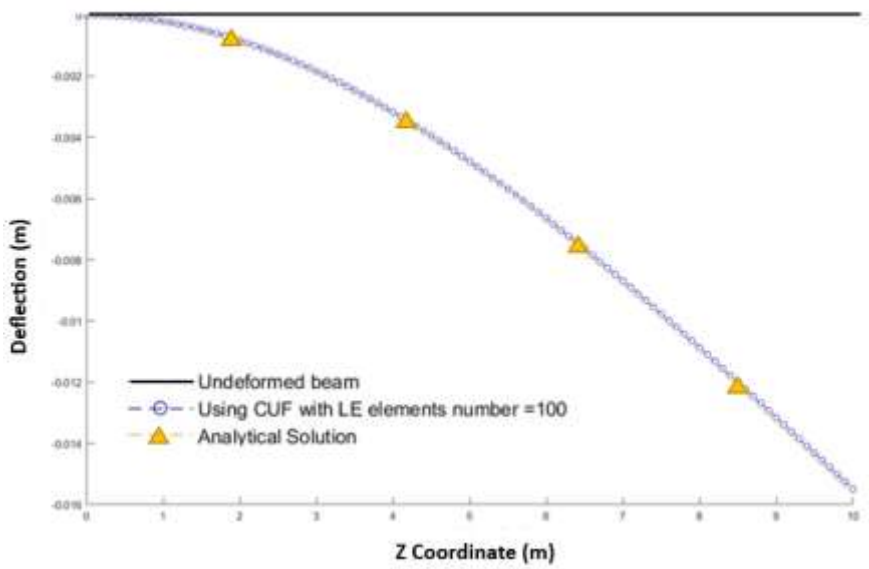

Figure 31. A comparison between a deformed 5-layer beam analyzed by CUF and discretized with 100 2L4 elements using quadratic axial shape functions and a deformed crack-free beam analyzed analytically.

In the beginning, the layers' number was held to 5 and the results with 100 and 200 5L4 elements and axial shape functions are shown in Figure 31 and Figure 32 respectively. The results are in good agreement with the analytical solution.

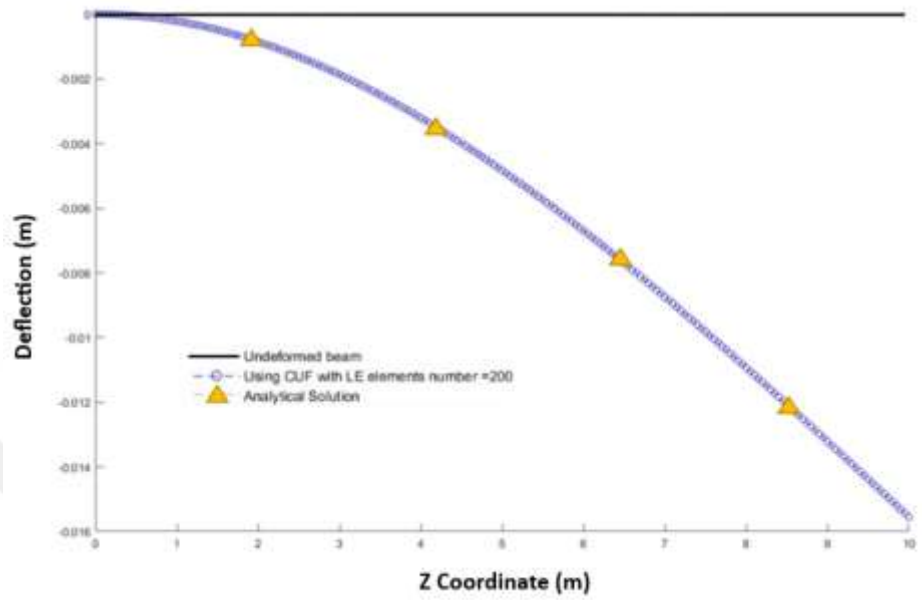

Figure 32. A comparison between a deformed 5-layer beam analyzed by CUF and discretized with 200 2L4 elements using quadratic axial shape functions and a deformed crack-free beam analyzed analytically.

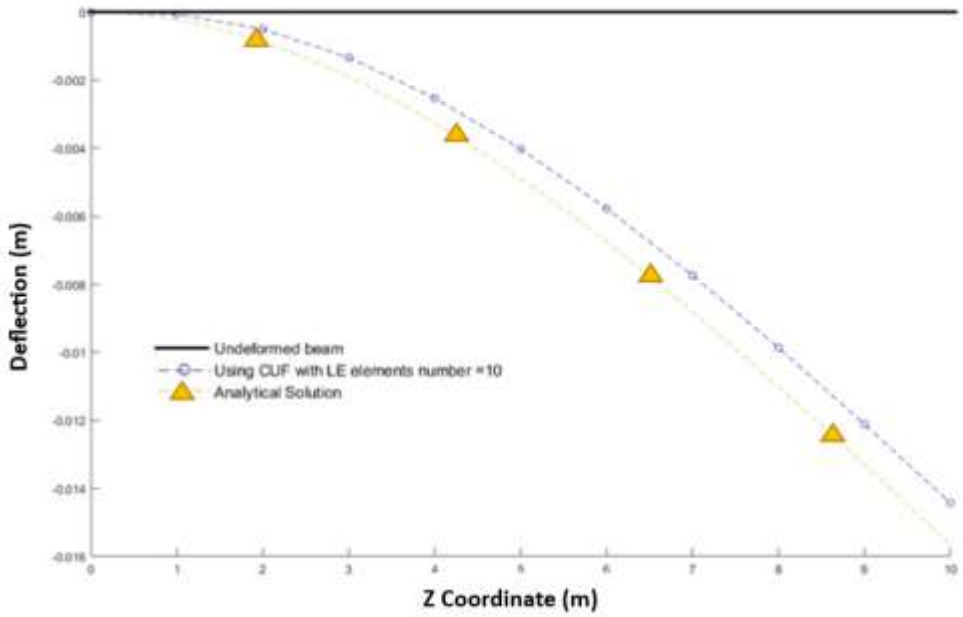

Figure 33. A comparison between a deformed 10-layer beam analyzed by CUF and discretized with 10 2L4 elements using quadratic axial shape functions and a deformed crack-free beam analyzed analytically.

We continue doing the verification with a beam of 10 layers. This code will be used later for our delamination simulation. We keep holding the material the same in all layers so it can be compared to single material beam analytical solution. The results of the analyses using 10, 40 and 60 (10L4) elements are shown in Figures 33, 34 and 35 respectively. It is noticed that the precision is increased with higher elements number.

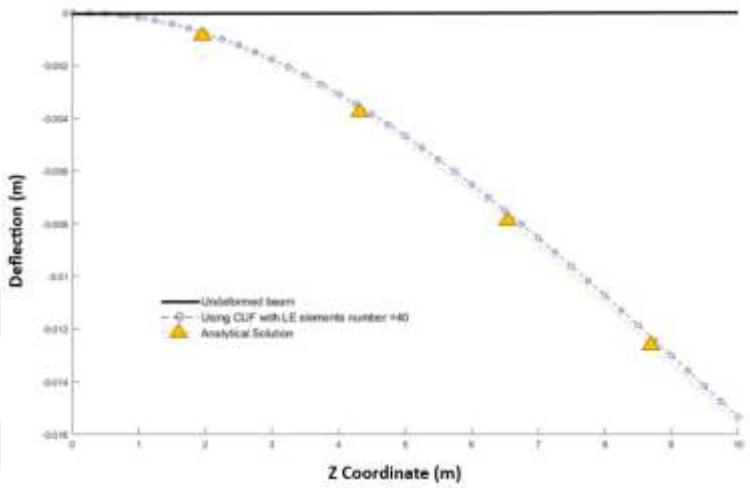

Figure 34. A comparison between a deformed 10-layer beam analyzed by CUF and discretized with 40 2L4 elements using quadratic axial shape functions and a deformed crack-free beam analyzed analytically.

In Figure 35, the results show full agreement with the analytical result. In the next section, 2 different materials will be given in the code as described in our original problem.

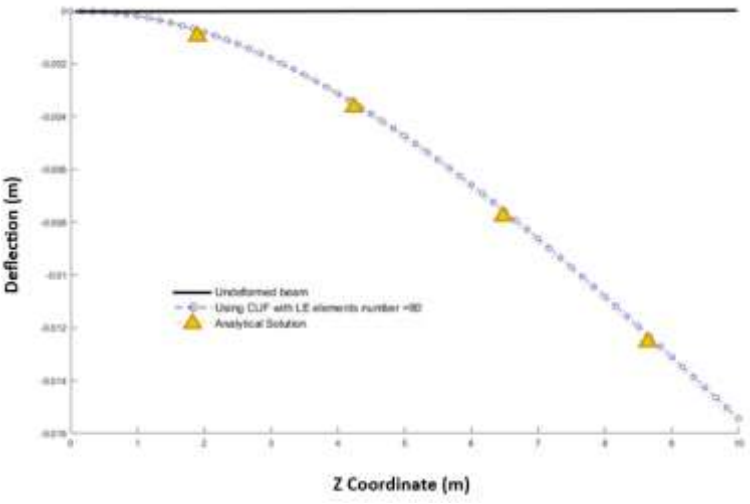

Figure 35. A comparison between a deformed 10-layer beam analyzed by CUF and discretized with 60 2L4 elements using quadratic axial shape functions and a deformed crack-free beam analyzed analytically.

Table 2. Deflections at the center point of the free end and errors for different numbers of elements when verification is applied on the 10-layer beam

Number of Layers	Number of Elements	Deflection at the Edge (CUF)	Deflection at the Edge (Analytically)	Error
10	10	0.0144	0.01563	%7
10	40	0.01533	0.01563	%1.9
10	60	0.01543	0.01563	%1.2

These results demonstrated in Table 2 are showing that the method used can give precise results and the accuracy can increase by using higher number of elements.

3.2 Bending of The FGM Beam Using CUF

In Figure 36, The bending of the beam with 5 layers discretized to 100 (5L4) elements is analyzed using different values for exponential constant n. A comparison is made between all the results and the analytical results of pure metal and pure ceramics beam.
The same last comparison is repeated on 10-layer beam with n=0.05 and n=10. The results are shown in Figure 37.

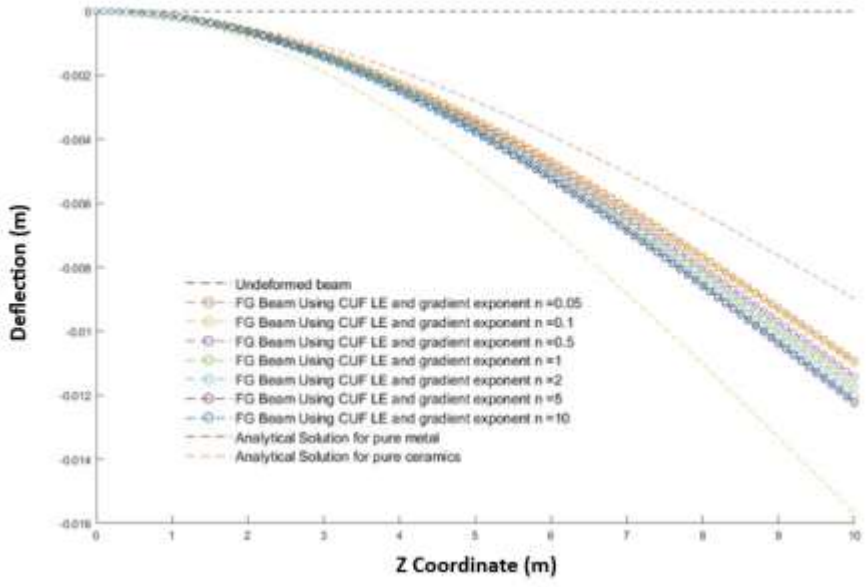

Figure 36. A comparison between deformed 5-layer FGM beams with different n factors analyzed by CUF and discretized with 100 2L4 elements using quadratic axial shape functions and deformed crack-free beams (pure metal and pure ceramics) analyzed analytically.

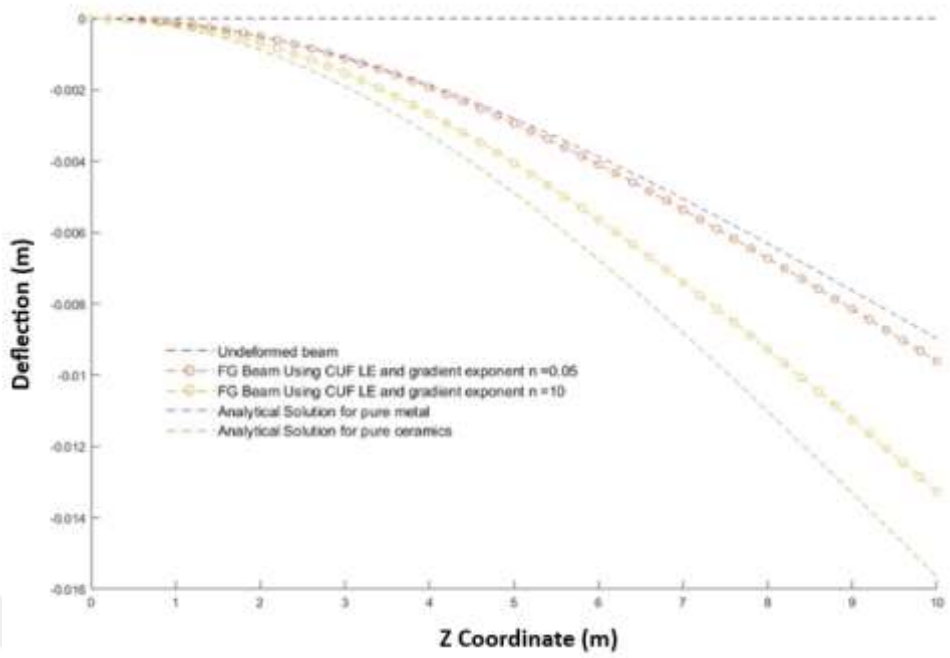

Figure 37. A comparison between deformed 10-layer FGM beams with different n factors analyzed by CUF and discretized with 50 2L4 elements using quadratic axial shape functions and deformed crack-free beams (pure metal and pure ceramics) analyzed analytically.

It is noticed that the factor (n) effect lose significance out of a specific range. The results approach the pure metal and the pure ceramic behavior as n goes further from 1, but doesn't totally intersect because one of the layers keeps its different metallic or ceramic properties. This difference decreases with the increased number of layers.

3.3 Delamination of The FGM Beam Using CUF and CZM

Lastly, to get the delamination simulation the forces (one upward on the upper layer and one downward on the lower layer) are applied gradually and the stiffness matrix is refreshed according to the displacements in the cohesive zone. In other words, the traction-separation law is conducted. The values of traction-separation law for each cohesive region of the 9 should have been determined by experimental tests. For simplicity the values were assumed and held the same in every cohesive region of the nine. In future studies, the values are planned to be taken by experimental tests on 3D printed samples when analyzing delamination of PLA-ABS FGM beams.

In this simulation the force was divided to 15 and the result was added every step till the 15th step. So the force increased gradually from zero among the first 15 steps till it reaches its maximum at the 15th step. 25 Total steps were used in the simulation. In the last 10 steps the force was constant. The simulation reached a static state in the last few steps.

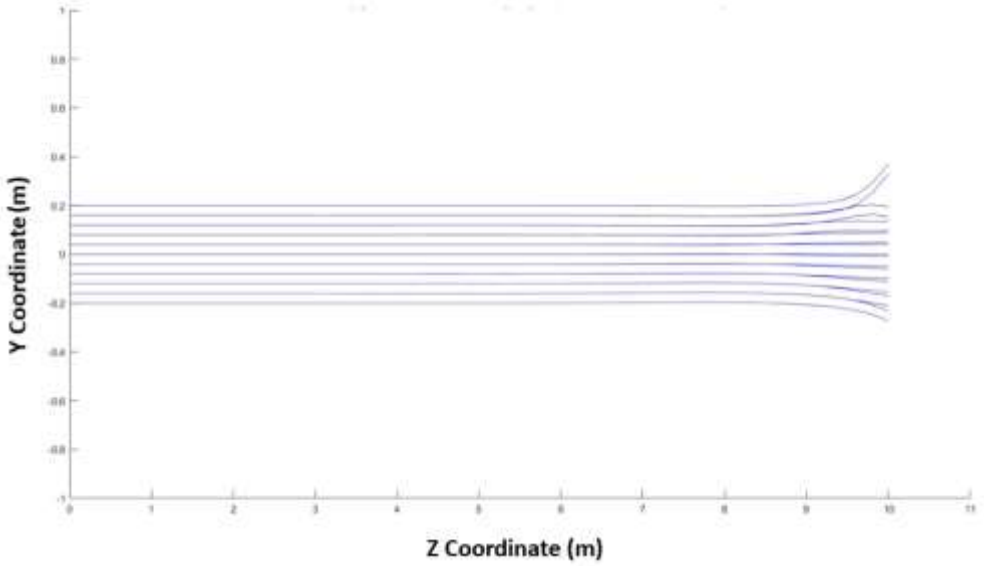

Figure 38. 1st sketch of the delamination analysis for 10-layer FGM beam using CZM and CUF 50 elements type 10L4 and quadratic axial shape functions.

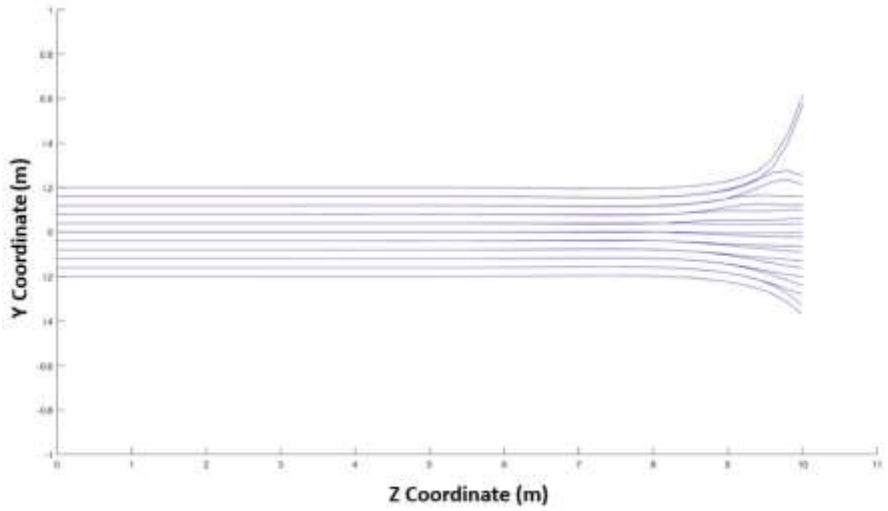

Figure 39. 2nd sketch of the delamination analysis for 10-layer FGM beam using CZM and CUF 50 elements type 10L4 and quadratic axial shape functions.

In Figures 38,39,40 and 41 there are four different sketches of our delamination problem of a 10-layer FG beam subjected to two forces acting on the edge layers in opposite direction forcing the beam to delaminate. The sketches were presented in a temporally order. CUF and CZM schemes were used for this solution. 50 (10L4) elements were employed with quadratic axial shape functions. It is noticed from the analysis that the metal rich region shows more deformation because of its higher ductility. In the future studies experimental delamination tests of the FGM beam may be run to over approve the results of this numerical scheme.

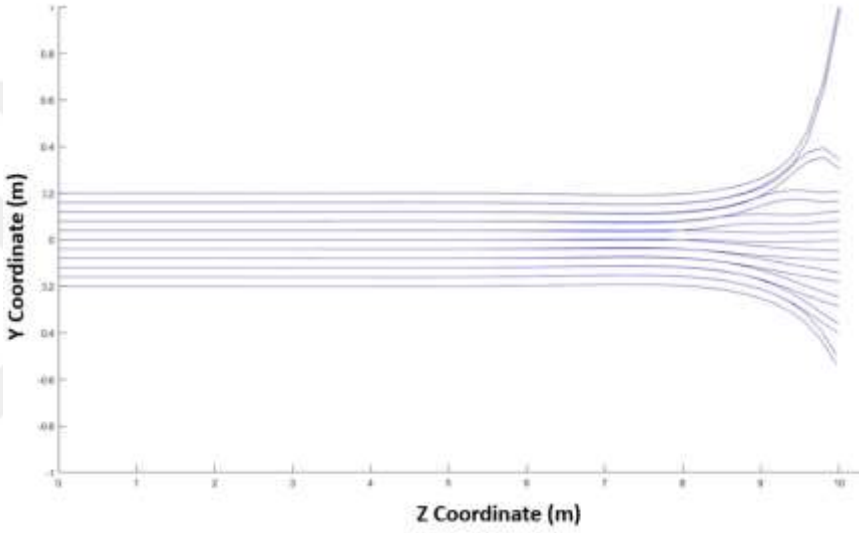

Figure 40. 3rd sketch of the delamination analysis for 10-layer FGM beam using CZM and CUF 50 elements type 10L4 and quadratic axial shape functions.

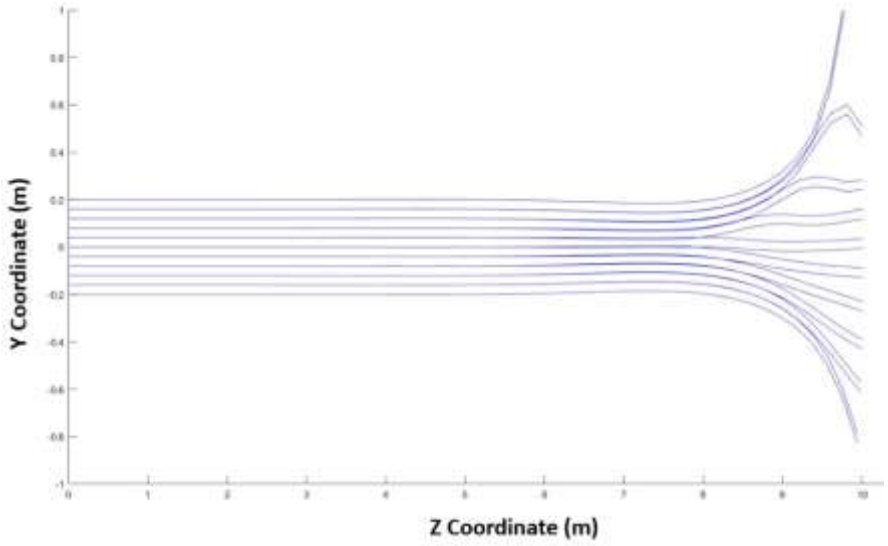

Figure 41. 4th sketch of the delamination analysis for 10-layer FGM beam using CZM and CUF 50 element

4. CHAPTER

DISCUSSION-CONCLUSION and RECOMMENDATIONS

4.1. Discussion

This thesis developed and analyzed functionally graded ceramic-metal (FGM) composite beams utilizing the CUF and CZM. FGM has great importance for engineering applications, especially in aerospace and automotive. The FGM composite has improved strength, toughness, and fatigue resistance by merging the mechanical properties of ceramics and metals.

CUF analyzed FGM composite fractured beams well. It is able to handle complex geometries and effectively simulate layered structures by applying Lagrange expansion. We simulated FGM composite beam delamination using the CZM. The CZM simulate interfacial behavior and failure mechanisms. This capacity is vital for analyzing FGM composite component structural integrity and durability under varied stress conditions.

4.2. Conclusion and Recommendations

Functionally graded ceramic-metal composites can revolutionize the design and manufacturing of high-performance structures by making them safer, more efficient, and environmentally friendly. That is why analyzing their behavior under different loading conditions is important. Mori-Tanaka scheme was used for determining mechanical properties in the laminates. CZM simulated the behavior of interlaminar region. Using CUF provides us with the flexibility needed for fracture analyses like delamination in our case. In the future, adding geometrical nonlinearity effect may improve the results reliability especially for cases when large displacement occur.

REFERENCES

1. Naebe, M., & Shirvanimoghaddam, K., 2016. Functionally graded materials: A review of fabrication and properties, **Applied materials today** (5): 223-245.
2. Shi, H., Zhou, P., Li, J., Liu, C., & Wang, L., 2021**.** Functional gradient metallic biomaterials: techniques, current scenery, and future prospects in the biomedical field, **Frontiers in Bioengineering and Biotechnology** (8): 616845.
3. Koizumi, M. F. G. M., 1997. FGM activities in Japan, **Composites part b: engineering** (28(1-2)): 1-4.
4. M. B. Bever, and P. E. Duwez, 1972. Gradients in composite materials, **Mater. Sci. Eng.** (vol. 10): pp. 1–8. DOI: 10.1016/0025-5416(72)90059-6.
5. M. Koizumi, 1993. Functionally gradient materials the concept of FGM, **Ceram. Trans.** (vol. 34): pp. 3–10.
6. T. Mori, and K. Tanaka, 1973. Average stress in matrix and average elastic energy of materials with misfittings inclusions**, Acta Metall.** (vol. 21: no. 5): pp. 571–574. DOI: 10.1016/0001-6160(73)90064-3.
7. Kumar, P., Sharma, S. K., & Singh, R. K. R., 2023. Recent trends and future outlooks in manufacturing methods and applications of FGM: a comprehensive review, **Materials and Manufacturing Processes** (38(9)): 1033-1067.
8. Watari, F., Omori, M., Hirai, T., Yokoyama, A., Matsuno, H., Uo, M., ... & Kawasaki, T., 2000. Fabrication and properties of FGM for biomedical application**. Journal of the Japan Society of Powder and Powder Metallurgy** (47(11)): 1226-1233.
9. Miyamoto, Y., Niino, M., & Koizumi, M. (1997). FGM research programs in Japan—from structural to functional uses, **In Functionally Graded Materials** (pp. 1-8). Elsevier Science BV
10. Demirbas, M., 2023. Thermo-elastic response of 2D-FGRPs with temperature-dependent material properties by means of the theory of elasticity, **Mechanics of Advanced Materials and Structures** (30:3): 520-542, DOI: 10.1080/15376494.2021.2018632.

11. M. K. Apalak, and M. D. Demirbas, 2020. Improved mathematical models of thermal residual stresses in functionally graded adhesively bonded joints: A critical review, Prog**. Adhesion Adhes.** (vol. 5): pp. 367–415.
12. K. Swaminathan, D. T. Naveenkumar, A. M. Zenkour, and E. Carrera, 2014. Stress, vibration and buckling analysis of FGM plates state-of-art review, **Compos. Struct.** (vol. 120): pp. 10–31, 2015. DOI: 10.1016/j.compstruct.2014.09.070.
13. J. N. Reddy, and C. D. Chin, 1998. Thermomechanical analysis of functionally graded cylinders and plates, **J. Therm. Stress.** (vol. 21, no. 6): pp. 593–626, DOI: 10.1080/01495739808956165.
14. Demirbas, M. D., Xu, X., Carrera, E., Yang, H., & Augello, R., 2020. Evaluation of stress distributions in the geometrical nonlinear regime of functionally graded structures. **Composite Structures** (246): 112385.
15. Demirbas MD, et al., 2020. Evaluation of the bending response of compact and thin-walled FG beams with CUF**.** Mech Adv Mater Struct :1–10.
16. M. M. Nemat-Alla, 2003. Reduction of thermal stresses by developing two dimensional functionally graded materials, Int**. J. Solids Struct.** (vol. 40, no. 26): pp. 7339–7356, 2003. DOI: 10.1016/j.ijsolstr.2003.08.017.
17. H. T. Thai, and S. E. Kim, 2015. A Review of theories for the modeling and analysis of functionally graded plates and shells, **Compos. Struct.** (vol. 128): pp. 70–86.
18. V. N. V. Do, and C. H. Thai, 2017. A modified Kirchhoff plate theory for analyzing thermo-mechanical static and buckling responses of functionally graded material plates**, Thin-Walled Struct.** (vol. 117): pp. 113–126, 2017. DOI: 10.1016/j.tws.2017.04.005.
19. I. M. Mudhaffar, A. Tounsi, A. Chikh, M. A. Al-Osta, M. M. Al-Zahrani, and S. U. Al-Dulaijan, 2021. Hygro-thermo-mechanical bending behavior of advanced functionally graded ceramic metal plate resting on a viscoelastic foundation, **Structures** (vol. 33): pp. 2177–2189, 2021. DOI: 10.1016/j.istruc.2021.05.090.
20. M. A. Rachedi, S. Benyoucef, A. Bouhadra, R. B. Bouiadjra, M. Sekkal, and A. Benachour, Impact of the homogenization models on the thermoelastic response of FG plates on variable elastic foundation, **Geomech. Eng.** (vol. 22, no. 1): pp. 65–80.

21. J. L. Mantari, and E. V. Granados, 2015. A refined FSDT for the static analysis of functionally graded sandwich plates, **Thin-Walled Struct.** (vol. 90): pp. 150–158, 2015. DOI: 10.1016/j.tws.01.015.
22. H. S. Shen, Y. Xiang, F. Lin, and D. Hui, 2017. Buckling and postbuckling of functionally graded graphene-reinforced composite laminated plates in thermal environments, **Compos. Part B. Eng.** (vol. 119): pp. 67–78. DOI: 10.1016/j.compositesb.2017.03.020.
23. M. W. Zaitoun, et al., 2022. Influence of the visco-Pasternak foundation parameters on the buckling behavior of a sandwich functional graded ceramicmetal plate in a hygrothermal environment, **Thin-Walled Struct.** (vol. 170): pp. 108549, DOI: 10.1016/j.tws.2021.108549.
24. S. I. Tahir, A. Chikh, A. Tounsi, M. A. Al-Osta, S. U. Al-Dulaijan, and M. M. Al-Zahrani, 2021. Wave propagation analysis of a ceramic-metal functionally graded sandwich plate with different porosity distributions in a hygro-thermal environment, **Compos. Struct.** (vol. 269): pp. 114030. DOI: 10.1016/j.compstruct.2021.114030.
25. Boğa, C., & Selek, O. N. U. R., 2020. Stress analysis of functionally graded beams due to thermal loading. **Journal of Engineering Science and Technology** (15(1)): 054-065.
26. Cem, B. O. Ğ. A., 2020. Effect of inhomogeneity constant on equivalent stresses in elastic analysis of hollow cylinder made from functionally graded material. **Gazi University Journal of Science** (33(1)): 201-212.
27. Knoppers, G. E., Gunnink, J. W., Van Den Hout, J., & Van Vliet, W. , 2005. December). The reality of functionally graded material products. In Intelligent Production Machines and Systems: *First I* PROMS Virtual Conference*, Elsevier (Amsterdam):(pp. 467-474).
28. S Wisnom MR., 2012. The role of delamination in failure of fibre-reinforced composites. **Philos Trans R Soc A:** Math, Phys Eng Sci (370):1850–70.
29. De Moura, M. F. S. F. ,2015. Application of cohesive zone modeling to composite bonded repairs. **The Journal of Adhesion** (91(1-2)): 71-94.
30. Dugdale DS. ,1960. Yielding of steel sheets containing slits. **Journal of the Mechanics and Physics of Solids** (8(2)):100-104.

31. Barenblatt GI. ,1962. The mathematical theory of equilibrium cracks in brittle fracture. **Advances in Applied Mechanics** (7):55-129.
32. Tvergaard V., 1990. Effect of fibre debonding in a whisker-reinforced metal. **Materials Science and Engineering** (A125(2)):203-213.
33. Xu Q, Tao W, Qu S, Yang Q. ,2015. A cohesive zone model for the elevated temperature 17 interfacial debonding and frictional sliding behaviour. **Composites Science and Technology** (110):45-52.
34. Alfano G, Crisfield MA., 2001. Finite element interface models for the delamination analysis of laminated composites: mechanical and computational issue. **International Journal for Numerical Methods in Engineering** ;(50(7)):1701-1736.
35. Feng D, Aymerich F., 2014. Finite element modelling of damage induced by low-velocity impact on composite laminates. **Composite Structures** (108):161-171.
36. Yang QD, Thouless MD., 2001. Mixed-mode fracture analyses of plastically-deforming adhesive joints. **International Journal of Fracture** (110(2)):175-187.
37. Jousset P, Rachik M. , 2014. Comparison and evaluation of two types of cohesive zone models for the finite element analysis of fracture propagation in industrial bonded structures. **Engineering Fracture Mechanics** (132):48-69.
38. Balzani C, Wagner W., 2008. An interface element for the simulation of delamination in unidirectional fiber-reinforced composite laminates. **Eng Fract Mech** (75):2597–615.
39. Benzeggagh ML, Kenane M., 1996. Measurement of mixed-mode delamination fracture toughness of unidirectional glass/epoxy composites with mixed-mode bending apparatus. **Compos Sci Technol** (56):439–49.
40. Turon A, Davila CG, Camanho PP, Costa J., 2007. An engineering solution for mesh size effects in the simulation of delamination using cohesive zone models. **Eng Fract Mech** (74(10)):1665–82.
41. Eijo A, Oñate E, Oller S., 2013. A numerical model of delamination in composite laminated beams using the LRZ beam element based on the refined zigzag theory. **Compos Struct** (104):270–80.
42. Nguyen VP, Kerfriden P, Bordas SPA., 2014. Two-and three-dimensional isogeometric cohesive elements for composite delamination analysis. **Compos Part B: Eng** (60):193–212.

43. Yuan, X. W., Li, W. G., Xiao, Z. M., & Zhang, Y. M., 2023. Prediction of temperature-dependent transverse strength of carbon fiber reinforced polymer composites by a modified cohesive zone model. **Composite Structures, (**304): 116310.
44. Huang, J., Zhang, C., Wang, J., & Zhang, C., 2022. On the applicability of rate-dependent cohesive zone models in low-velocity impact simulation. **Engineering Fracture Mechanics, (**271): 108659.
45. Marulli, M. R., Valverde-González, A., Quintanas-Corominas, A., Paggi, M., & Reinoso, J., 2022. A combined phase-field and cohesive zone model approach for crack propagation in layered structures made of nonlinear rubber-like materials. **Computer Methods in Applied Mechanics and Engineering,** (395): 115007.
46. Linke, M., & Lammering, R., 2023. On the calibration of the cohesive strength for cohesive zone models in finite element analyses. **Theoretical and Applied Fracture Mechanics,** (124): 103733.
47. Chiachio, M., Chiachio, J., Saxena, A., & Goebel, K., 2016. An energy-based prognostic framework to predict evolution of damage in composite materials. In Structural health monitoring (shm) in aerospace structures (pp. 447-477). Woodhead Publishing.
48. Safri, S. N. A. B., Sultan, M. T. H., & Jawaid, M., 2019. Damage analysis of glass fiber reinforced composites. In Durability and life prediction in biocomposites, fibre-reinforced composites and hybrid composites (pp. 133-147). Woodhead Publishing.
49. Kora, S., & Gorantla, N., 2023. A review on delamination and wear characteristics of metal matrix composites. *In AIP Conference Proceedings* (Vol. 2759, No. 1). AIP Publishing.
50. Huang, Y. J., Yang, Z. J., Zhang, H., & Natarajan, S., 2022. A phase-field cohesive zone model integrated with cell-based smoothed finite element method for quasi-brittle fracture simulations of concrete at mesoscale. **Computer Methods in Applied Mechanics and Engineering**, (396): 115074.
51. Ekhtiyari, A., & Shokrieh, M. M., 2022. A novel rate-dependent cohesive zone model for simulation of mode I dynamic delamination in laminated composites. **Composite Structures,** (281): 114962.

52. Wang, R., Liu, Y., Mao, J., Liu, Z., & Hu, D., 2022. Cyclic cohesive zone model damage parameter acquisition for fatigue crack growth considering crack closure effect. **International Journal of Fatigue,** (163): 107021.
53. Huo, X., Luo, Q., Li, Q., Zheng, G., & Sun, G., 2022. On characterization of cohesive zone model (CZM) based upon digital image correlation (DIC) method. **International Journal of Mechanical Sciences,** (215): 106921.
54. Lecinana, I., Zurbitu, J., Renart, J., & Turon, A., 2023. A robust fatigue parameter determination method for a local fatigue cohesive zone model. **International Journal of Fatigue, (**171):107582.
55. Xu, X., Wang, D., Zang, M., & Chen, S., 2022. Development of an intrinsic solid-shell cohesive zone model for impact fracture of windshield laminated glass. **International Journal of Impact Engineering,** (163): 104187.
56. Li, R., Xu, Z., Zou, X., Hu, C., & He, X., 2023. A frictional cohesive zone model for characterizing transverse compression responses of unidirectional fiber-reinforced polymer composites. **Mechanics of Advanced Materials and Structures,** (30(11)): 2164-2172.
57. Yang, Z., Yang, H., Wang, L., & Cao, D., 2023. The development and application of an interfacial cohesive zone model of the pavement interlayer considering the characteristics of adhesive materials. **Case Studies in Construction Materials, (**18): e01775.
58. Fu, C., & Wang, X., 2022. Simulating delamination in composite laminates involving large scale fiber bridging based on the mixed-mode three-linear cohesive zone model. **Theoretical and Applied Fracture Mechanics**, (117): 103164.
59. Bhandari, M., & Purohit, K., 2022. Dynamic fracture analysis of functionally graded material structures–a critical review. **Composites Part C: Open Access**, (7): 100227.
60. Kumar, D., Budarapu, P. R., & Pradhan, A. K., 2023. Numerical analysis of lap shear joints made of functionally graded materials. **Journal of the Brazilian Society of Mechanical Sciences and Engineering,** (45(2)): 94.
61. Pascuzzo, A., Greco, F., Ammendolea, D., Lonetti, P., & Gaetano, D., 2022. On the combination of Moving Mesh technique and M-integral method for predicting

crack propagation mechanisms in Functionally Graded Materials. **Procedia Structural Integrity,** (39): 649-662.

62. Han, D., Liu, G., Yang, T., Xie, Y., & Zhao, Y., 2023. A phase-field cohesive zone model for fracture simulation of asphalt mixture. **Engineering Fracture Mechanics,** (281): 109149.
63. Muc, A., 2022. Buckling of Composite Structures with Delaminations—Laminates and Functionally Graded Materials. **Applied Sciences**, (12(22)): 11408.
64. Rahimi, M. N., & Moutsanidis, G., 2022. Modeling dynamic brittle fracture in functionally graded materials using hyperbolic phase field and smoothed particle hydrodynamics. **Computer Methods in Applied Mechanics and Engineering**, (401): 115642.
65. Kaleel, I., Carrera, E., & Petrolo, M., 2020. Progressive delamination of laminated composites via 1D models. **Composite Structures,** (235): 111799.
66. Khoramishad, H., Hamzenejad, M., & Ashofteh, R. S., 2016. Characterizing cohesive zone model using a mixed-mode direct method. **Engineering Fracture Mechanics,** (153): 175-189.
67. Xu, X. P., & Needleman, A., 1993. Void nucleation by inclusion debonding in a crystal matrix. **Modelling and Simulation in Materials Science and engineering**, (1(2)): 111.
68. Carrera, E., Cinefra, M., Petrolo, M., & Zappino, E., 2014. Finite Element Analysis Of Structures Through Unified Formulation. John Wiley & Sons,416
69. Online materials information resource-MatWeb, **http://www.matweb.com** (access on October 2022)
70. Paulino, G., Jin, Z. H., & Dodds, R. H., 2007. 2.13-Failure of functionally graded materials. In Comprehensive structural integrity: pp. 607-644. Elsevier Ltd.
71. Mori, T., & Tanaka, K., 1973. Average stress in matrix and average elastic energy of materials with misfitting inclusions. **Acta metallurgica**, (21(5)): 571-574.

CURRICULUM VITAE

Personal Information

Name, Surname: Mohammed Nasseer Abdulrahman MOHAMMED

EDUCATION

Degree	**institution**	**Date of graduation**
Master's Degree	Erciyes University, Mechanical Engineering	2023
Master's Degree	Ruhr University Bochum, Computational Engineering	-
Bachelor's Degree	Erciyes University, Mechanical Engineering	2020

Foreign Languages

English - Turkish - German